High-field EPR of bioorganic radicals

Stefan Stoll[a]
DOI: 10.1039/9781849730877-00107

1 Introduction

More and more enzymes are being discovered that involve protein-, cofactor- or substrate-based radicals in their catalytic cycles.[1–3] These bioorganic radicals serve either as redox-active intermediaries in electron transfer over long distances, or as reactive cofactors that perform chemical tasks such as hydrogen abstraction. They also occur as paramagnetic substrate intermediates in sometimes stunningly acrobatic radical transformations. The lifetimes of these radicals vary widely. Some are stable over hours, and others can be freeze-trapped on the second, millisecond or microsecond time scales. There are transient radicals with an existence so fleeting that it has so far been impossible to observe them.

The study of the structure of bioorganic radicals is crucially important for understanding enzymatic reaction mechanisms and the inner working of electron transfer in proteins. This understanding is relevant for designing analogous de novo systems. Bioorganic radicals have therefore received close attention from EPR spectroscopists. Alongside traditional continuous-wave (cw) EPR at X-band (9–10 GHz, about 0.3–0.4 T), high-field cw EPR has been deployed to examine bioorganic radicals and the details of their electronic and geometric structure. High-field EPR encompasses magnetic field strengths beyond about 2 T, where conventional resistive magnets are not able to generate fields sufficiently homogeneous for acquiring unbroadened radical EPR spectra. The corresponding frequencies lie above about 60 GHz.

The main structural parameter that can be obtained from the high-field EPR spectrum of an organic radical is the g tensor, characterized by its three principal values g_x, g_y, g_z along three orthogonal molecule-fixed directions (principal axes). The associated g shifts, i.e. the deviations of these g values from the g value of the free electron, $g_e = 2.002319\ldots$, contain valuable information about the chemical nature of the radical, its protonation state, its total charge, its conformational state, the presence or absence of hydrogen bonds, and the polarity of the radical's microenvironment. The main advantage of high-field EPR over X-band EPR is the increased g or Zeeman resolution, i.e. the increased capability of resolving resonances with only slightly different g factors, allowing accurate measurement of the three principal values of the g tensor.

There are additional benefits of high-field EPR. The resolution of the g tensor results in increased orientational selectivity. In a disordered system such as a powder or a frozen solution, only radicals with a small subset of orientations are resonant with the microwave frequency at a set magnetic field. In contrast, at X-band usually all orientations are resonant at the same

[a]*Department of Chemistry, University of California Davis, One Shields Ave, Davis, CA 95616, U.S.A.*

field. This increased orientational selectivity of high-field EPR is advantageous for experiments performed at constant field like ENDOR (electron-nuclear double resonance), ESEEM (electron spin echo envelope modulation) and PELDOR (pulsed electron-electron double resonance). The field dependence of the resulting spectra reveals additional valuable information. The benefits of high-field EPR are by no means restricted to biological organic radicals. Other radicals such as nitroxides are studied as well. They are used as spin labels in biological systems, and with high-field EPR the proticity and polarity of the label's microenvironment[4] as well as fast time scales of motional processes can be probed.[5] Last but not least, the power of high-field EPR is widely used to study high-spin systems with large zero-field splittings.

Aspects of the application of high-field EPR to the study of organic radicals in biological systems were reviewed several times in the last few years.[6–10] Recently, an impressive book dedicated to high-field EPR, its instrumentation and several important biological systems has appeared.[11]

In comparison to the wide applicability and diversified methodology of high-field EPR, this review is very limited. It concentrates on g tensors of biological organic radicals relevant in enzymology, as obtained by high-field cw or echo-detected EPR. Not included are ENDOR, time-resolved EPR and PELDOR studies of the same radicals. This review focuses on the major bioorganic radicals with available g tensor data, but also mentions, without attempt for completeness, some biological radicals of current interest for which g tensors have not yet been reported.

There are two obvious systematic ways to organize bioorganic radicals: either by the biological system (protein) they are associated with or by their chemical nature. Neither approach is entirely satisfactory, and either results in a certain degree of repetition, as certain radicals occur in many proteins and certain proteins harbour many different radicals. The second one has been chosen here and coarsely groups the radicals into protein-derived amino acid radicals, cofactor radicals and substrate radicals, even though amino acid radicals often can be thought of as cofactors, and non-amino acid cofactors might be covalently bound to the protein. The subdivision is blurry and slightly arbitrary, but unavoidable.

2 The g tensor

This initial section summarizes theoretical aspects of the g tensor relevant to the analysis of high-field EPR spectra of organic radicals and the interpretation of the g tensor. Very clear introductions to the g tensor can be found in the exquisite classic textbooks by Carrington and McLachlan[12] and by Atherton.[13]

2.1 Orientation dependence of g

The g value of a free electron is $g_e = 2.002319\ldots$[14] and describes the interaction of the magnetic moment of the electron with the external magnetic field. When the electron is confined in a molecule, the magnetic field at which resonance occurs at a given frequency becomes dependent on the orientation of the molecule with respect to the magnetic field. When the

orientation of the radical in the magnetic field is changed, the resonance line shifts. In other words, the g factor is generally different from g_e, and it is anisotropic. Its deviation from g_e, termed the *g shift*, is analogous to chemical shift and shielding in NMR.

Resonance occurs when the microwave frequency ν_{mw} and the magnitude B of the magnetic field $\boldsymbol{B}$ satisfy the resonance condition

$$h\nu_{mw} = \mu_B g(\boldsymbol{n}) B \tag{1}$$

(where h is the Planck constant, and μ_B is the Bohr magneton). Here, $g(\boldsymbol{n})$ is the orientation-specific g factor, and $\boldsymbol{n} = \boldsymbol{B}/B$ is the orientation of the magnetic field relative to the molecule. Expressed in polar angles θ (away from the z-axis of the molecule-fixed frame) and ϕ (anticlockwise from x in the xy plane of the molecule-fixed frame), it is $\boldsymbol{n}^T = (\sin\theta\cos\phi, \sin\theta\sin\phi, \cos\theta)$.

2.2 Spin Hamiltonian description

In the spin Hamiltonian, this anisotropic magnetic interaction between the unpaired spin in the electronic ground state of the radical and the external magnetic field is described by the electron Zeeman term:

$$H_{EZ} = \mu_B \boldsymbol{B}^T \boldsymbol{g} \boldsymbol{S} \tag{2}$$

where $\boldsymbol{S}$ is a 3-element vector operator with the elements S_x, S_y and S_z, representing the (fictitious) electron spin angular momentum and $\boldsymbol{g}$ is the 3×3 matrix representing the g tensor.

The g tensor in Eq. (2) summarizes the orientation dependence of the g factor. $g(\boldsymbol{n})$ can be obtained from the g tensor using:

$$g(\boldsymbol{n}) = \left|\boldsymbol{n}^T \boldsymbol{g}\right| = \sqrt{\boldsymbol{n}^T \boldsymbol{g}\boldsymbol{g}^T \boldsymbol{n}} \tag{3}$$

from which it is clear that $g(\boldsymbol{n})$ depends on the product $\boldsymbol{g}\boldsymbol{g}^T$ (sometimes denoted as $\boldsymbol{G}$, Γ, or $\boldsymbol{g}^2$) and not on $\boldsymbol{g}$. Mathematically, the matrix of the product $\boldsymbol{g}\boldsymbol{g}^T$ is symmetric even if the matrix $\boldsymbol{g}$ is asymmetric. Consequently, a potential intrinsic asymmetry in $\boldsymbol{g}$ does not affect the line positions and cannot be determined from cw EPR spectra. $\boldsymbol{g}$ (as opposed to $\boldsymbol{g}\boldsymbol{g}^T$) is therefore experimentally not uniquely defined.[15,16] Usually, the antisymmetric component of $\boldsymbol{g}$ is very small in organic radicals.

The g tensor obtained via spectral analysis is always the symmetrized tensor $\boldsymbol{g}_{sym} = (\boldsymbol{g}\boldsymbol{g}^T)^{1/2}$. It yields the same spectra as $\boldsymbol{g}$. The three eigenvalues and three eigenvectors of $\boldsymbol{g}_{sym}$ constitute the three experimental principal g values and the associated principal axes. Conventionally, these are labelled such that their principal values are ordered $g_x \geq g_y \geq g_z$.

Quantum chemistry programs (e.g. the generally available ORCA, Gaussian, and ADF) compute and often return an asymmetric $\boldsymbol{g}$. It can be used directly in spectral simulations if the simulation software allows it,[17] or $\boldsymbol{g}_{sym}$ can be used instead.

2.3 Physical origin

The interaction between the spin and the magnetic field described by Eq. (2) can be pictured in two ways, either as the interaction of the total magnetic moment of the radical $-\mu_B \boldsymbol{g}\boldsymbol{S}$ with the external magnetic

field $\boldsymbol{B}$, or as the interaction between the spin-only magnetic moment $-\mu_B g_e \boldsymbol{S}$ with the total magnetic field $\boldsymbol{B}^T \boldsymbol{g}/g_e$, externally applied plus locally induced.

The first model is the common one. It starts by considering the effect of the spin on the ground state wave function in the absence of the external magnetic field. The spin perturbs the ground state wave function compared to the spin-free case through spin-orbit coupling, such that the spin-including ground state is different from the spin-free one. With the help of perturbation theory, the ground state is described as a small admixture of excited electronic states to the original (spin-free) ground state. The g tensor results from the interaction of this wave function with the magnetic field. This treatment goes back to the original work of Pryce on the g tensor of atoms,[18] but was first developed for organic π radicals with delocalized spin density by Stone.[19,20]

In general, the deviation of the g tensor from g_e is a sum over three terms:

$$\boldsymbol{g} = \boldsymbol{g} - \boldsymbol{g}_e = \boldsymbol{g}_{RMC} + \boldsymbol{g}_{GC} + \boldsymbol{g}_{SO} \tag{4}$$

where $\Delta\boldsymbol{g}_{RMC}$ is the small isotropic and negative relativistic mass correction (the electron's mass is larger when it moves),[21] and $\Delta\boldsymbol{g}_{GC}$ is a usually small diamagnetic gauge correction term.[19] The last term $\Delta\boldsymbol{g}_{SO}$, the paramagnetic spin-orbit/orbit Zeeman term, is the largest and therefore most important contribution. If $\boldsymbol{g}$ is significantly shifted from g_e, it is due to this last term. It can be approximated as a sum of individual contributions from all atoms in the molecule. The contribution of a given atom is proportional to its spin-orbit coupling constant, its share of unpaired ground state spin density, and the populations of excited states that are rotationally related to the ground state. It is inversely proportional to the energy difference between the ground and the excited states.

This is best illustrated by the example in Fig. 1. In a phenoxy radical, the unpaired spin in the singly occupied molecular orbital (SOMO) is delocalized over the six carbon π orbitals of the benzene ring, but also onto the π ($2p_z$) orbital of the oxygen. The oxygen additionally has in-plane non-bonding orbitals, of which one is schematically shown in Fig. 1. When the magnetic

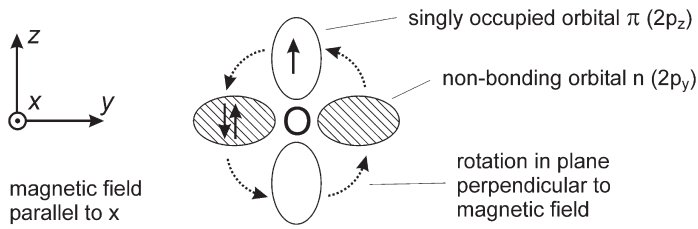

Fig. 1 Schematic illustration of the rotational relation between a singly occupied anti-bonding π orbital (such as out-of-plane $2p_z$ on the oxygen in the phenoxy radical) and the orthogonal doubly occupied non-bonding orbital (such as in-plane $2p_y$ on the oxygen in the phenoxy radical). The C–O bond and magnetic field vector point out of the paper plane. The rotation is orthogonal to the field.

field is directed parallel to the C–O bond (x-axis), the corresponding g value shift contribution from the oxygen is:

$$g_{\mathrm{SO},x}(\mathrm{O}) = \frac{2\zeta_{\mathrm{O}}\rho_{\pi}^{\mathrm{O}}c_{\mathrm{ny}}^{2}}{E_{n\pi}}. \quad (5)$$

ζ_{O} is the spin-orbit coupling constant of a 2p electron on the oxygen atom. ρ_{π}^{O} is the population of the singly occupied orbital, and c_{ny}^{2} is the contribution of the in-plane orbital $2p_y$ to the excited state resulting from promotion of one of its electrons to the π orbital. This excited state contributes to the g shift, since the resulting SOMO (the n orbital) is rotationally related to the SOMO of the ground state in a way indicated by the arrows in Fig. 1. $\Delta E_{n\pi}$ is the energy difference between the excited state and the ground state.

All the factors in Eq. (5) can vary and determine the g shift. First and foremost is the spin-orbit coupling constant. It scales approximately with the fourth power of the nuclear charge. An often referenced representative set of approximate values is (C = 28, N = 76, O = 151, S = 382 cm^{-1}),[12] but others are quoted as well.[22,23] A very comprehensive table is found in Blume's 1963 article.[24] Without ζ, the g tensor in organic π radicals would be a non-local "bulk" property of the unpaired spin density distribution, since every atom contributes to a shift according to Eq. (5). However, with ζ, it is biased towards non-carbon atoms like oxygen. This bias is enhanced by the fact that the oxygen in-plane lone pair orbitals are energetically closer to the SOMO than the in-plane orbitals of the carbons, which are involved in covalent bonding.

The nonbonding orbitals can be energetically stabilized by hydrogen bonds and by being placed in a polar environment. As a consequence, $\Delta E_{n\pi}$ increases and $\Delta g_{\mathrm{SO},x}$ decreases. This environmental effect on the in-plane g values of an organic π radical allows us to use the in-plane values of the g tensor as reporters not only on the chemical nature of the radical, but also on its protonation state, its hydrogen bonding network, and the polarity of its microenvironment. The out-of-plane g value g_z, on the other hand, is of little diagnostic value in π radicals, since the spin-orbit contribution is essentially zero due to the lack of appropriate low-lying excited states with the required rotational behaviour.

The second way to look at the phenomenon of the g tensor is more classically inspired, but is equally suited for quantitative computations. In this, the spin of the unpaired electron is initially disregarded. When a molecule is placed in a magnetic field, charge currents are induced in the electron density distribution. If there are unpaired spins, spin currents will arise as well.[25,26] The arrows in Fig. 1 illustrate this spin current. The (spin-free) ground state wave function in the presence of the field is therefore not the same as in a field-free situation. In a frame of reference fixed on the moving unpaired electron, the electric fields due to the charges of nuclei and the other electrons appear as additional magnetic fields. The interaction of the spin of the unpaired electron with these internal magnetic fields is equivalent to the spin-orbit coupling and results in the deviation of g from g_e. When the orientation of the molecule with respect to the external field is changed, the induced spin currents change, and so does the g value.

Due to the importance of the spin-orbit coupling in determining the g tensor, its accurate computation in quantum chemical programs is crucial and has received much attention. The older simple semiempirical ansatz of effective nuclear charges[27] has now been replaced by implementations of the spin-orbit mean-field approach, a quantitatively better model that takes two-electron contributions into account.[28]

2.4 g resolution

Let us examine more closely the enhanced g resolution at high field mentioned in the introduction. The three g values g_x, g_y, g_z correspond to resonances at three fields B_x, B_y, B_z, with:

$$B_x = \frac{h\nu_{mw}}{\mu_B} \cdot \frac{1}{g_x} \text{ etc} \tag{6}$$

for a given spectrometer frequency ν_{mw}. Resonance lines with two slightly different g factors, say g_x and g_z, are therefore separated by:

$$B_g = B_z - B_x = \frac{h\nu_{mw}}{\mu_B}\left(\frac{1}{g_z} - \frac{1}{g_x}\right) \approx B_0 \frac{g_x - g_z}{g_0} \tag{7}$$

where g_0 is the mean of the two g values, $g_0 = (g_x + g_z)/2$, and B_0 is the corresponding resonance field, $B_0 = h\nu_{mw}/\mu_B\, g_{iso}$. In a powder sample, ΔB_g quantifies the spectral broadening due to the anisotropy of the g tensor. In addition to this g broadening, the spectrum is broadened by the resolved and unresolved splittings due to hyperfine couplings between the unpaired electron spin and nearby magnetic nuclei, summarily denoted as ΔB_{hf}.

The g broadening/splitting ΔB_g is proportional to the field, whereas the hyperfine broadening ΔB_{hf} is field independent. Fig. 2 illustrates the

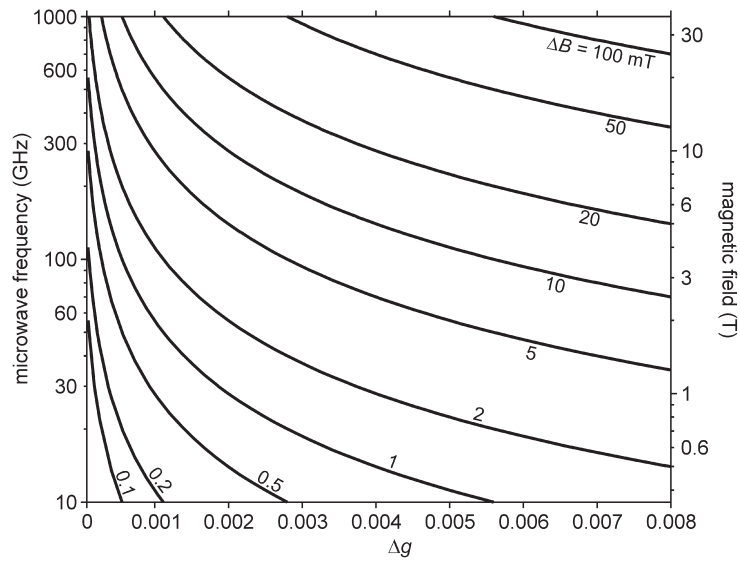

Fig. 2 Magnetic field separation ΔB_g resulting from two slightly different g values g_1 and g_2, around $g = 2.00$ as a function of their difference, $\Delta g = g_1 - g_2$, of the spectrometer frequency and of the magnetic field.

dependence of ΔB_g on the difference Δg between two g values around $g = 2$, as a function of the spectrometer frequency and the magnetic field. For a tyrosyl radical with $\Delta g = 0.005$, the field separation at 100 GHz is about 9 mT, clearly above the hyperfine broadening of < 5 mT. On the other hand, a chlorophyll radical with $\Delta g = 0.001$ gives a separation of only 2 mT at the same frequency, clearly not enough to dominate the hyperfine broadening of about 2 mT. At low field, e.g. at X-band, ΔB_{hf} is much larger than ΔB_{g} for both radicals. Hyperfine splitting and broadening dominates the spectrum, and the g tensor is obscured.

For visibly resolving at least the largest and smallest principal value of the g tensor, the g broadening must be significantly larger than the hyperfine broadening:

$$\Delta B_{\mathrm{g}} > \Delta B_{\mathrm{hf}}. \tag{8}$$

In this case, the effects of the hyperfine broadening do not obscure the g anisotropy, and the g tensor can be easily determined from the spectrum. This condition of g or Zeeman dominance is sometimes invoked as defining the high-field regime in EPR.[11] Δg_{xy} and Δg_{yz} are smaller than Δg_{xz}, so that even higher fields are needed to resolve the g values. Since high-field EPR spectra resolve the g tensor, they are orientation selective and therefore sensitive to the relative orientation between various anisotropic hyperfine tensors and the g tensor.

The condition of g or Zeeman dominance in Eq. (8) cannot only be reached by going to higher field and increasing ΔB_{g}, but also by reducing ΔB_{hf} via perdeuteration of the radical.[29–37] This can reduce ΔB_{hf} by up to a factor of $|g_{\mathrm{n}}(^1\mathrm{H})/g_{\mathrm{n}}(^2\mathrm{H})| = 6.5$, and consequently a smaller increase of ΔB_{g} is necessary to potentially resolve the g tensor. Especially in radicals with very narrow g tensors, this has proven essential to achieve complete separation of the three principal values at available high fields, e.g. for chlorophyll-based radicals at 130–140 GHz.[38–40] Note however that in several types of radicals (flavins, tryptophans) nitrogen couplings significantly contribute to ΔB_{hf}. An isotope substitution of ^{14}N by ^{15}N would reduce the number of hyperfine lines from 3 to 2, but does not result in substantial spectral narrowing, as $3\ |g_{\mathrm{n}}(^{14}\mathrm{N})| \approx 2\ |g_{\mathrm{n}}(^{15}\mathrm{N})|$.

Spectral lines can also be narrowed by using crystals instead of powders or frozen solutions. This eliminates the Zeeman broadening, although site splitting might be present.[13] Single crystals have been used since the very early days of high-field EPR[41] and continue to yield valuable insight into electronic structure by revealing the g tensor orientation in the molecule if the crystal structure is known. At Q-band, the g tensor of a quinone radical could be resolved in a single crystal study using perdeuteration.[32] Several groups have published high-field EPR single-crystal studies: e.g. on the primary donor radical in bacterial reaction centers,[42,43] on the tyrosyl D radical in photosystem II,[44] on the tyrosyl radical in ribonucleotide reductase[45,46] (all at 95 GHz), and on the biliverdin substrate radical in phycocyanobilin:ferredoxin oxidoreductase[47] (at 130 GHz).

When ΔB_{hf} and ΔB_{g} are similar in magnitude, spectra are broadened and often hard to interpret. In the low-field limit, ΔB_{hf} dominates ΔB_{g}, the spectral shape is determined by the hyperfine couplings only, and the

relative tensor orientations have no effect. This low-field limit is, however, not completely reached for many radicals at X-band. For instance, 9.5 GHz spectra of tyrosyl and tryptophan radicals are asymmetric as a result of ΔB_g. This asymmetry is visually obvious when the spectrum is overlaid with a copy of itself that is flipped left-right and up-down.

For high-accuracy simulations at X-band, even g tensors as small as (2.0035, 2.0030, 2.0020), typical for tryptophan radicals, have to be taken into account. Omission of a correct g tensor in the analysis increases the uncertainty in the determination of the hyperfine coupling constants. Additionally, the relative orientations of the tensors can play a role. Therefore, it is crucial to independently and reliably determine the g tensors from high-field spectra, not only for learning about molecular structure from its principal values, but also in order to be able to correctly extract hyperfine data from low-field spectra. Vice versa, if all relevant hyperfine couplings are known accurately from the analysis of ENDOR spectra, the g tensor can sometimes be estimated from X-band or Q-band spectra using careful spectral simulation.[33,48] It is, however, not straightforward to assess the errors associated with the determined g tensor principal values.

Low-field EPR spectra without Zeeman dominance are useful for determining the magnitude of the hyperfine couplings. In tyrosyl and tryptophan radicals, these are related to the side chain orientation. In favourable cases, they allow the distinction between a Trp and a Tyr radical from low-field EPR[49], although the g tensor is more reliable as discussed below.

3 Experimental aspects

The current state of the art in high-field EPR instrumentation has been summarized in several recent reviews.[11,50] See also the regular reviews by Smith in this series.[51] In the context of this overview, a short discussion of experimental aspects relevant to high-field EPR of bioorganic radicals is given. The commonly used frequency and field conditions are summarized, and the issues of sensitivity, field calibration and g value accuracy are considered.

3.1 Frequency ranges

Although the first high-field EPR studies that were able to resolve the g anisotropy of an organic radical were done in the 1950s (e.g. on 2,2-diphenyl-1-picrylhydrazyl crystals at 75 GHz[41]), it took until the 1990s before high-field EPR became routinely available. The development was strongly driven by the interest in bioorganic radicals. For an excellent historic overview, see Möbius.[11]

Nowadays, the most common spectrometer frequency for high-field EPR is in the W-band at approximately 94–95 GHz, mostly due to its commercial availability. Above W-band, there exist several home-built setups that are used to acquire organic radical spectra, e.g. at 130 GHz (D-band),[40,47,52,53] 140 GHz[38,54–56] and 180 GHz (G-band).[57] There are quite a few spectrometers that can go beyond 200 GHz, e.g. 244 GHz,[58] 245 GHz,[59] 250 GHz,[60] 275 GHz[61] and 285 GHz (3×95 GHz).[62]

In the very-high-frequency range above about 300 GHz, spectra of organic radicals have been acquired in a 360 GHz/12.8 T setup in Berlin.[63,64] At the National High Magnetic Field Laboratory in Tallahassee, a homodyne transmission setup with a 17 T superconducting magnet has been used extensively to acquire bioorganic radical spectra at up to 416 GHz/14.8 T. Higher fields can be obtained by pumping, and a spectrum obtained at 437 GHz/15.7 T has been published.[65] This is the current technical limit for sweepable superconducting magnets with sufficient homogeneity. Also, it is the upper limit of frequencies that solid state sources can generate with sufficient power.

To reach higher fields, resistive Bitter magnets are used. They require several megawatts of power and large amounts of cooling water. In Tallahassee, a high-homogeneity Bitter magnet can achieve fields up to 25 T, and radical spectra have been acquired at frequencies close to 700 GHz using either a far-infrared laser[66–68] or a backward wave oscillator[69] as source. In Grenoble, spectra at 525 GHz/18.7 T have been obtained using a Bitter magnet and a far-infrared laser.[70] The upper limit in field is given by the difficulty of generating stable and homogeneous magnetic fields with accurate linear sweeps. Also, THz sources with sufficiently high power and stability are not yet easily available.

3.2 Sensitivity

At high field/frequency, the intrinsic properties of the resonators can yield increased sensitivity for small samples. This is an important advantage of high-field EPR over low-field EPR, since frozen solution samples with biological radicals are often limited in concentration and volume. Proteins can often only be handled or are available only at concentrations well below 1 mM and in small volumes. Often, bioorganic radicals are only minority species, so that their actual concentration can be an order of magnitude or two lower than the protein concentration. For single crystal studies, high sensitivity is crucial, as protein crystals often have very small volumes in the nanoliter range.

When high-frequency resonators such as cylindrical cavities and Fabry-Pérot structures are used, the samples are necessarily small, and the increased sensitivity of high-field EPR is needed. However, not all setups use resonant structures to take advantage of it. Non-resonant ''bucket'' systems are used for example in Grenoble,[59] Saclay,[62] Tallahassee[71] and St. Andrews.[72] They compensate their lower sensitivity by accommodating large sample volumes up to 1 mL. They have important advantages over small resonant structures. Sample handling and loading in darkness and under liquid nitrogen is easier, samples can be degassed, and a field standard can easily be added to the sample. However, single-crystal studies are not possible.

3.3 Field calibration

Accurately measuring EPR spectra of organic radicals crucially requires accurate knowledge of both the frequency and the field. The frequency is held constant during an EPR experiment, and for most types of microwave sources, it is stable and either known or can otherwise be measured very

accurately. In contrast, the magnetic field is varied. Magnetic fields are difficult to produce and control. Accurate values of the magnetic field are therefore less easily obtained.

High-field EPR places several demands on the magnets and their power supplies: high homogeneity, multi-digit stability, and sweep linearity. Due to hysteresis effects in magnets, it is not sufficient to measure the current to determine the magnetic field. Rather, the field should be measured directly, ideally at the same point in time and space where the EPR sample experiences it. Optimally, an NMR teslameter based for example on the accurately known proton magnetic moment[73] is used within the high-homogeneity region of a magnet.[74] A new NMR-based precision field-sweep system for high-field EPR was developed[37] and applied[75] recently, but such devices are not generally available and cannot be placed in the homogeneous field region in every setup.

Therefore, secondary paramagnetic standards are widely used to calibrate the magnetic field. These are samples with known magnetic parameters and are placed into or next to the EPR sample container together with the sample and provide spectra with known line positions from which an accurate magnetic field axis can be derived. The magnetic parameters of these standards are determined at low fields using high-precision NMR teslameters and magnets with very good field homogeneities over a large region. The two most common standards are LiF:Li and MgO:Mn^{2+}. LiF:Li contains small metallic nanoclusters of Li that are generated by high-intensity neutron irradiation of LiF crystals. They feature an extremely narrow metallic resonance line with isotropic $g = 2.002293(2)$ at room temperature.[76,77] The spectrum of MgO:Mn^{2+} exhibits six hyperfine lines with isotropic $g = 2.00101(5)$ and $A = -243.9(1)$ MHz.[78–80] Other standards occasionally used include P-doped Si (featuring one line with $g = 1.9985$ at high P donor concentrations, and two lines separated by 4.4 mT at low donor concentration),[32,81–83] 2,2-diphenyl-1-picrylhydrazyl (DPPH),[84–86] potassium nitrosodisulfonate (Frémy's salt),[40,87] perdeuterated tempone,[88] aromatic hydrocarbon radicals such as the perylene radical cation,[89] and K_3CrO_8.[90] Recently, atomic hydrogen trapped in octaalkylsilsesquioxane, a silicate nanocage,[91,92] was proposed as a standard.[93] The endohedral hydrogen atom is created by γ-irradiation of the silicate cage material and is surprisingly stable at room temperature. Its spectrum consists of two isotropic lines separated by about 50 mT. It has an isotropic g value of 2.00294(3) and a slightly temperature dependent isotropic hyperfine coupling constant between $+1416.8(2)$ MHz below 70 K to $+1413.7(1)$ MHz at room temperature.[93] Its two lines do not overlap with the spectra of organic radicals.

3.4 Accuracy

Using the secondary standards, the experimental accuracy of g tensor principal values that can be obtained by high-field EPR is generally reported to be between 0.00002 to 0.00020 for absolute g values, and 2–10 times better for the differences $g_x - g_y$ etc.

The difference error depends mostly on spectral fitting errors due to large linewidths, low signal-to-noise ratio, partial overlap of g features and

incomplete spin Hamiltonian models. Unfortunately, the difference error is not always specified.

The much larger error in the absolute values is due to a combination of the uncertainty in the magnetic parameters of the field standards, of field offsets between standard and sample, and of lineshape distortions due to fast-passage effects and absorption/dispersion admixture. The latter can sometimes be alleviated by a Hilbert transform.[94] Estimates of systematic errors due to spatial and temporal separation between standard and EPR sample acquisition are not available, even though they are clearly present. This can be seen by comparing g values from radicals that have been studied in several high-field EPR laboratories, e.g. the tyrosyl D radical in photosystem II or the primary donor radical in bacterial reaction centres.

The best practically attainable absolute accuracy for g values is currently two orders of magnitude worse than the known accuracy of the fundamental constants involved in spectral analysis using Eq. (1). In the latest set of recommended fundamental constants,[73] the relative uncertainties of h and μ_B are $5 \cdot 10^{-8}$ and $2.5 \cdot 10^{-8}$, respectively. In this context, it is worthwhile mentioning that the measurement accuracy of the g factor of the free electron was substantially improved several times in recent years[14] to an astonishing $2.8 \cdot 10^{-13}$ relative, using a 150 GHz one-electron quantum cyclotron.

Given the accuracy gap to the fundamental constants and the lab-to-lab spread in g values of the same system, one must say that the problem of reproducibly and accurately measuring absolute g values in high-field EPR is currently not entirely solved.

4 Comparison of g tensors of biological radicals

The systematic dependence of the g tensor of organic radicals on the nature of the radical and its microenvironment is best appreciated in a two-dimensional plot that graphs the *skew* or *anisotropy* of each g tensor against its *span*. If the three principal axes of the g tensor are labelled such that the principal values are ordered $g_x \geq g_y \geq g_z$, the span and skew are given by:

$$\text{span} = g_x - g_z \quad \text{skew} = \frac{g_x - g_y}{g_x - g_z} \tag{9}$$

The span describes the anisotropy of the g tensor and the width of the powder spectrum. The skew characterizes the rhombicity of the g tensor and thereby the asymmetry of the spectrum. For axial g tensors, the skew is either zero or one, and it is 0.5 for a fully rhombic one.

Definitions of span and skew similar to Eq. (9) are used in NMR to characterize chemical shift and shielding tensors.[95] The skew is similar to an intermediate parameter used by Svistunenko in his analysis of tyrosyl spectra.[96] Differences of g values have been tabulated by Angerhofer in a review of chlorophyll radicals.[97] Christoforidis[98] used $(g_x - g_z)/g_z$ as a measure for the anisotropy.

There are two rationales behind the choice of span and skew for a two-dimensional plot: (1) Both are based on differences of g values, which have much smaller experimental errors than the absolute g values, as discussed

above. Therefore, the differences result in a more reliable graph than a plot of absolute values against each other (as done for example for g tensors of nitroxide radicals in the pioneering work of Lebedev[99]). (2) Essentially all organic radicals in biology are π radicals. According to Stone theory, the out-of-plane g value of such radicals is always very close to g_e and is therefore not diagnostic of the radical or its environment. If its deviation from g_e is correlated to molecular structure, it is too small for current levels of experimental accuracy to allow a systematic study (for an exception, see Petrenko[83]). Taking g_z as a baseline in the differences in span and skew therefore eliminates one of the three variables without sacrificing physical content.

The scan/skew plot is shown in Fig. 3. It contains a representative number of published experimental g tensors, all of them determined by high-field EPR between 95 and 670 GHz. Clearly, the g tensors of a given type of radical are clustered. The g tensors of tyrosyl radicals constitutes the largest set. The dependence of both g_x and g_y on the microenvironment is evident from the large distribution in span, while at the same time the skew is more or less conserved. Tyrosyl radicals with large spans are located in hydrophobic pockets, and hydrogen bond and polar environments cause the g tensor to shrink and move to the left in the plot. Flavin radicals can be either neutral or anionic, and from the plot it can be seen that the main difference stems from the skew, while the anisotropy/span is not affected. All chlorophyll radicals have similarly tiny spans, but their g_y values vary substantially. The few data points for tryptophan radicals are also grouped together, although they are currently too few to allow insight into microenvironmental effects. It seems that the skew is more variable than the span.

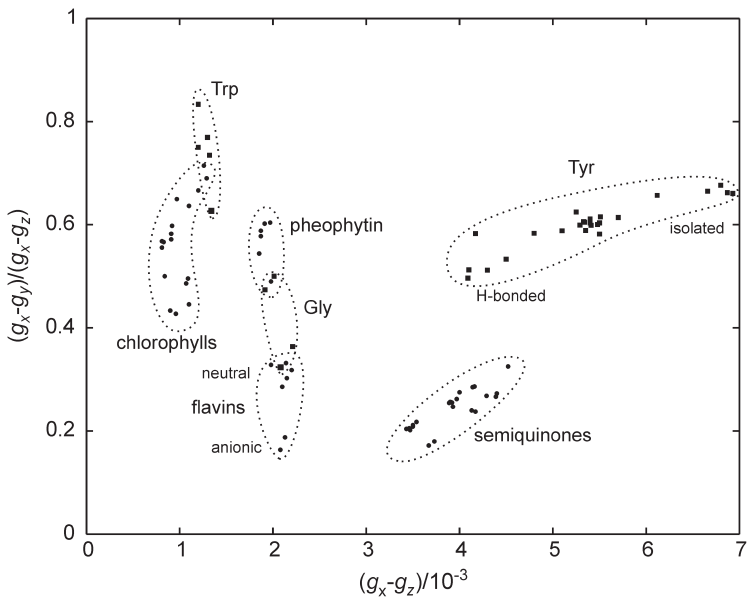

Fig. 3 Comparison of some published experimental g tensors of common biological organic radicals based on the span $g_x - g_z$ and the skew $(g_x - g_y)/(g_x - g_z)$ of the g tensors, with $g_x \geq g_y \geq g_z$.

For all the radicals, however, the g tensor is at least a fingerprint property of their chemical nature, and the plot can serve as a convenient reference.

One aspect to keep in mind is that g tensor measurements are done at different temperatures, and the g tensors in some systems can be temperature dependent due to motional effects or electronic exchange phenomena. The regions in the plot in Fig. 3 therefore not only illustrate static effects on $\boldsymbol{g}$ from charge, hydrogen bonds or polarity, but they are also potentially affected by dynamic effects.

5 Amino acid radicals

The common protein-based amino acid radicals are shown in Fig. 4. By far the most widespread and well studied is the tyrosyl radical, but systems with tryptophan radicals are increasingly being examined. Radicals on the other two canonical aromatic amino acids, histidine and phenylalanine, have not been observed *in vivo*. Their redox potentials are probably out of reach for physiological oxidants. Cysteinyl and glycyl radicals are rare, but serve important functions as hydrogen abstracting agents. Recently, modified tyrosines have been incorporated into proteins, and the corresponding oxidized radicals have been observed. All these radicals are π radicals; that is, the unpaired spin resides in orbitals that are normal to a molecular plane, and in-plane lone pairs are present on some atoms. In the following, we examine each of the types of radicals in turn, mention the systems in which they occur and summarize their high-field EPR results.

5.1 Tyrosyl radicals

The most commonly observed organic radical in proteins is tyrosyl, resulting from one-electron oxidation and deprotonation of tyrosine (see Fig. 5). There are many proteins that form stable or transient tyrosyl radicals.[100,101] Tyrosine often serves as crucial mediator in electron transfer. It participates in redox processes via proton-coupled electron transfer,[102] where it transfers its phenolic proton to a nearby proton acceptor upon donating an electron to an acceptor. The redox potential of tyrosine is tuned by the protein microenvironment. In contrast to tyrosine's importance for electron transfer, its role in other chemical transformations is very limited.

The two most important systems with stable Tyr radicals are photosystem II and ribonucleotide reductase,[103] which catalyze processes absolutely central to life. In many other systems, transient tyrosyl radicals can be

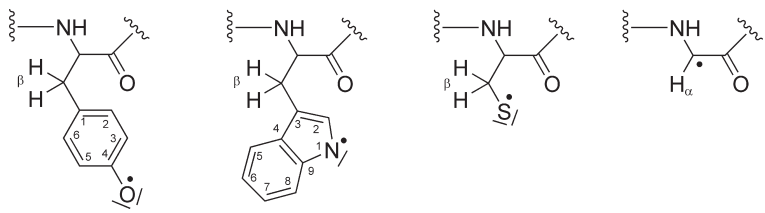

Fig. 4 The protein-based amino acid radicals tyrosyl, tryptophanyl, cysteinyl, and glycyl. They are obtained by one-electron oxidation and deprotonation of the respective amino acids. Only one resonance structure is shown.

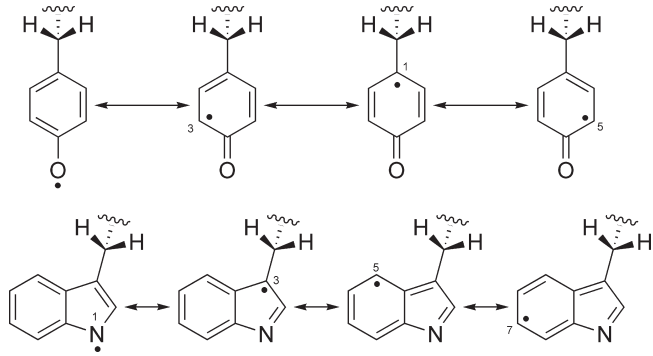

Fig. 5 Major resonance structures of the neutral radicals of tyrosine (top) and tryptophan (bottom). On tyrosyl, the spin density is concentrated on the phenoxy oxygen and on ring carbons 1, 3 and 5. On the tryptophan radical, it is mainly on the indole nitrogen and on ring carbons 3, 5 and 7.

induced in mutants or under non-physiological turnover conditions and trapped by rapid freeze quench, suggesting them as catalytic intermediates. Often, these tyrosyl radicals are off-pathway, i.e. they do not play a role in the catalytic cycle. Although the biochemical relevance of some of these tyrosyl radicals is therefore unclear, they are realistic model systems for studying the effect of the protein environment on magnetic parameters and can contribute substantially to the understanding of how proteins manage and tune their redox-active sites.

5.1.1 Photosystem II

Photosystem II (PS II) is the photosynthetic membrane protein complex that is responsible for converting light into chemical reducing equivalents, abstracting the necessary electrons from water and generating oxygen as a by-product. After absorption of a photon, a primary donor chlorophyll centre transfers an electron via a series of redox-active cofactors (pheophytin, plastoquinone Q_A) to a quinone cofactor (plastoquinone Q_B) that can dissociate from the complex. The oxidized primary donor fills the resulting hole by oxidizing the nearby tyrosine Y_Z (Y161 on the D1 subunit), which in turn regains its electron from the oxygen evolving complex (OEC), a Mn_4Ca cluster. Once the latter cluster has lost four electrons, it oxidizes two water molecules and produces oxygen. Y_Z is therefore the crucial secondary donor that enables electron transfer between water and the quinone Q_B. Its lifetime is in the microseconds range. On the other hand, another very stable tyrosyl radical is formed when PS II preparations are dark adapted. It is located on another tyrosine, Y_D (Y160 on the D2 subunit).[104]

Since $Y_D^{\cdot}$ is very stable, it was extensively studied by EPR. The g tensor was first derived from simulations of X- and Q-band spectra.[105,106] Its high-field EPR spectrum was first published in 1992,[107] and several subsequent high-field EPR studies,[56,103,108–110] including a single-crystal study at 95 GHz[44], accurately determined the g tensor in PSII from spinach and several cyanobacteria. Typical values are (2.0075, 2.0044, 2.0022). In Fig. 3, the measured values are clustered in the centre of the tyrosine region, with

an anisotropy of about 0.0053. These measurements are summarized in a 2001 review[62]. Since then, an interesting study demonstrated the generation and trapping of the tyrosyl D radical in its state prior to deprotonation by illumination at 1.8 K.[111] The g tensor was determined at 245 GHz. Consistent with theoretical expectations, the g_x value of the protonated form is substantially smaller (2.00643) than the one of the deprotonated form. A partial deprotonation could be observed by annealing the sample at 77 K, and deprotonation was complete after incubation at 200 K. The phenoxy group of tyrosine D is hydrogen bonded to a histidine (D2-His[189]). When this residue is mutated to glutamine, the g_x value increases to 2.00834[109], consistent with the expectations from Stone theory when the hydrogen bond is removed.

Despite the expansive research done on Y_D, it is still not clear what function this tyrosine serves in PS II. Since it is conserved among photosynthetic organisms, it is most likely not a "spurious" radical, but relevant for assembly, functioning or repair of PS II. Roles in photoactivation of the Mn_4Ca cluster or electrostatic regulation have been suggested. The various proposed functions of Y_D are discussed in a review appropriately entitled "Why D?".[104]

The much shorter lived radical on Y_Z has been more elusive. It can be obtained in a manganese-depleted PS II mutant that lacks Y_D (D2-Tyr160Phe). Its g tensor, determined at 245 GHz,[109] is almost identical to that of $Y_D^{\bullet}$. However, it was found that the g_x value is distributed, indicating a structural heterogeneity in the hydrogen bonding network around the phenoxy oxygen of the radical. At high pH, the g_x value decreases for unclear reasons.[62] Also, in Mn- and Ca-depleted PS II at low pH, $Y_Z^{\bullet}$ gives X-band EPR and ENDOR spectra different from those at neutral pH[112], indicating significant changes in the spin density distribution. As there are no high-field EPR data available yet, it remains to be determined whether this is due to protonation of the radical or to other changes in the microenvironment. The $Y_Z^{\bullet}$ radical can also be generated in preparations containing the Mn_4Ca cluster, yielding a split signal due to the coupling between the radical and the paramagnetic S_2 state of the cluster. The two g values 2.0069 and 2.0079 were deduced from 190 and 285 GHz spectra of the split signal.[113] In another recent study of $S_2Y_Z^{\bullet}$, a g_x value of 2.00689 was inferred.[114]

Model systems with a hydrogen bond similar to the one between tyrosine and histidine in PS II have been studied both theoretically and experimentally.[115–117]

5.1.2 Ribonucleotide reductase

The other very extensively studied tyrosyl radical is from ribonucleotide reductase (RNR).[118] RNR synthesizes the four deoxyribonucleoside triphosphates required for DNA replication and repair by reducing the 2′-OH group of the ribose subunit to 2′-H.[119] All RNRs employ a cysteine thiyl radical (see below) to initiate the reaction by abstracting 3′-H from the substrate. Different RNRs use different pathways to generate, store and transfer this radical. Class I RNRs use a tyrosyl radical, class II RNRs use a cobalamin-derived adenosyl radical, and class III RNRs use a glycyl radical

(see below). Class I RNRs contain two dimeric subunits. The thiyl radical in the active site in the catalytic subunit (α_2 or R1) is generated by long-range electron transfer via intermediate tyrosine residues to a tyrosyl radical in the vicinity of a μ-oxo-bridged di-iron centre in the cofactor subunit (β_2 or R2). The tyrosyl radical is generated by dioxygen via a high-potential oxidation state of the di-iron cluster.

The g tensor of the tyrosyl radical has been characterized in RNRs from *Escherichia coli* (Y122),[45,54,103,120–122] *Salmonella typhimurium* (Y105),[46,123] mouse (Y177),[120–122,124] herpes simplex virus type 1 (Y132),[120] *Mycobacterium tuberculosis* (Y110),[121,125] yeast[126] and *Arabidopsis thaliana* (Y125).[121,127] A low-field spectrum is available from *Bacillus anthracis*.[128] The g tensors fall into two distinct groups. For mouse, yeast and *A. thaliana*, the g_x values lie in the range 2.0075–2.0078. For *E. coli*, *S. typhimurium* and *M. tuberculosis*, they are larger with values between 2.0086 and 2.0092. There are therefore two types of environments for the RNR tyrosyl radical: one that facilitates hydrogen bonds in the higher organisms, and a more hydrophobic pocket in the others.[129] Interestingly, in one study the radical signal from *M. tuberculosis* RNR has been found to be a mixture of two signals, one with $g_x = 2.0080$ and one with $g_x = 2.0092$.[125,130]

High-field single-crystal cw EPR studies on the Tyr radical in RNR in comparison with X-ray structure of the reduced form revealed that upon oxidation the Tyr side chain moves slightly away from the di-iron centre in *E. coli* RNR,[45] but slightly closer to it in *S. typhimurium* RNR.[46]

RNR of *Chlamydia trachomatis* harbours a Mn-Fe site instead of the Fe-Fe site found in most other RNRs.[131] Also, the position of the Tyr radical is taken by Phe, and even after a Phe/Tyr mutation, no radical is obtained. Active RNRs with a Mn-Mn centre and a tyrosyl radical can be obtained in *E. coli*[132] and in *Corynebacterium glutamicum*.[133] A very recent detailed multi-frequency analysis[134] of the EPR spectrum of the tyrosyl radical exchange-coupled to the metal cluster in its $Mn^{III}Mn^{III}$ state yielded a g_x value of 2.0085.

The discoveries of the tyrosyl radicals in PS II and RNR have generated substantial interest in the effects of the microenvironment on the g tensor. Quantum chemical calculations at various levels of theory[103,109,115,135–137] have been used to study the influence of the environment and of hydrogen bonds on the tyrosyl g tensor. Already the early studies found that g_x is a measure of the electrostatic environment.[103,109,136,138] A least-squares fit to the results of semiempirical calculations on a model system gave an approximate dependence of g_x from the distance r between the phenoxy oxygen and the hydrogen of a hydrogen-bond donor[103,109] as:

$$g_x = 2.0094 - \frac{0.0033}{(r/\mathrm{A} - 0.5)^2}. \tag{10}$$

5.1.3 Haem enzymes. In addition to PS II and RNR, tyrosyl radicals occur in a host of haem enzymes. In the cytochrome P450 enzyme superfamily, catalysis proceeds via an intermediate state called "compound I", which consists of a high-valent [Fe(IV) = O] haem ($S = 1$) with a radical on the porphyrin, $P^{\bullet +}$. This state is generated from the Fe(III) heme resting

state by dioxygen and electrons from a reducing agent. In contrast, addition of external chemical oxidants (peroxides, peracids, iodosobenzene) can give rise to the formation of "compound ES" species, where the radical is not based on the porphyrin, but rather on the protein. Often, these radicals are tyrosines, and they have been studied by EPR. Examples include P450cam from *Pseudomonas putida* (CYP101),[139,140] P450BM3 from *Bacillus megaterum* (CYP102)[141] and prostacyclin synthase (also known as prostaglandin I_2 synthase, PGIS). For the tyrosyl radical in the last enzyme, a g_x value of 2.00970 has recently been measured at 130 GHz.[53] This is the highest g_x value of a tyrosyl radical known to date, indicating the absence of hydrogen bonding to the phenoxy oxygen and a completely hydrophobic pocket. The location of the radical is currently unknown.

Prostaglandin H_2 synthase (PGHS) is a key enzyme in the biosynthesis of prostaglandins and thromboxanes from arachidonic acid. It has peroxidase activity, and EPR spectra from a series of radicals (named "wide doublet" and "wide singlet") have been reported.[31,142] The peroxide-induced radicals are suggested to be located on Y385 and Y504 in the ovine enzyme.[143] High-field EPR studies[142,144] obtained g_x values between 2.0066 and 2.0068.

A tyrosyl-type radical has also been detected in the bifunctional KatG catalase-peroxidase from *M. tuberculosis*. KatG is a crucial enzyme that activates the antitubercular prodrug isoniazid. The radical is obtained after treatment with peracetic acid[145,146] and high-field EPR have been published.[147] KatG is also known to give rise to several tryptophan radicals, as discussed in the corresponding section.

When bovine liver catalase is treated with an excess of peracetic acid, a [Fe(IV) = O Tyr•] intermediate is formed.[148,149] Its g tensor was measured at 285 GHz, and a slight pH dependence of the g_x value was observed.[138]

Tyrosyl radicals have further been identified in a gamut of other heme peroxidases, e.g. lactoperoxidase,[150] the W191F mutant of cytochrome c peroxidase,[151] turnip peroxidase,[152] horseradish peroxidase mutant F172Y,[153] dehaloperoxidase[154,155] and, last not least, cytochrome c oxidase.[156,157] Tyrosyl radicals are observed in both the one- and two-electron activated forms of the Trp164Tyr mutant of *Pleurotus eryngii* versatile peroxidase[158,159] (see section on tryptophan radicals).

When haemoglobins and myoglobins are treated with H_2O_2, tyrosyl radicals are generated.[160] There is possibly a Tyr radical under turnover in oxalate decarboxylase.[161] A tyrosyl radical was also detected in the molybdopterin-containing enzyme xanthine oxidase after treatment with ferricenium at high pH.[162]

Some of the tyrosyl radicals in heme enzymes are not physiologically relevant, but their location relative to the active site can yield important insight into how proteins manage electrons.

5.1.4 Other systems

A transient tyrosine radical has been observed in (6–4) photolyase from *Xenopus laevis*.[163] It acts as the final electron donor to the flavin cofactor (see below). A similar radical has been observed in *Anacystis nidulans* cyclobutane pyrimidine dimer (CPD) photolyase.[164]

Radicals in γ-irradiated Tyr · HCl crystals have been studied for a long time,[165] and signals from both protonated cation and deprotonated neutral tyrosyl radicals have been observed[166]. However, only recently has high-field EPR been used to determine the g tensors more accurately. Maniero[167] identified three Tyr radicals in Tyr · HCl crystals γ-irradiated at room temperature, differing substantially in their g_x values (2.00621, 2.00661 and 2.00769) as a result of different hydrogen bonding environments around the phenoxy oxygen (two, two and one H-bond, respectively). In contrast, the radical observed in γ-irradiated N-acetyltyrosine is not hydrogen bonded. From 105 GHz EPR, a large g_x value of 2.0094(2) was derived.[168] This value is close to those of the radicals in RNR of *M. tuberculosis*, *E. coli* and *S. typhimurium* and in prostacyclin synthase, which are also above 2.009.

5.2 Tryptophanyl radicals

The spin density on the tryptophan radical is delocalized over the indole ring (see Fig. 5). The g tensors of tryptophan radicals are rather narrow, typical values being $g_x = 2.0033$–2.0036, $g_y = 2.0024$–2.0027, and $g_z = 2.0021$–2.0023. The span/anisotropy $g_x - g_z$ is about 4–5 times smaller than for tyrosyl radicals and $g_y - g_z$ is very small (0.0003-0.0005). The reduced g tensor anisotropy compared to Tyr is due to the absence of oxygen with its high spin-orbit coupling constant and to higher spin density on the ring carbon 3. Whereas tyrosyl g values are easily resolved at W band, tryptophan radicals require significantly higher fields for complete separation of the three principal values. Nevertheless, g values can be extracted from W-band spectra.

RNR. The first high-field EPR spectra of Trp radicals were observed in mutants of RNR.[33] Mutation of the tyrosine radical site 122 in *E. coli* RNR to Phe resulted in a Trp111 radical. When tyrosine at the analogous site 177 in mouse RNR was mutated to Trp, a Trp177 radical was obtained. The g tensors of these two Trp radicals were accurately determined at W-band[122] and are very similar.

Azurin. In the copper-containing electron transfer protein azurin from *Pseudomonas aeruginosa*, several Trp radicals have been observed. In one mutant, a surface-exposed Trp inserted at position 108 was generated by photolysis using a Re(I) photosensitizer attached to a histidine inserted at position 107. The radical was studied at 285 GHz, where the g tensor with principal values 2.00355, 2.00271 and 2.00221 is partially resolved.[169] Recently, another Trp radical, Trp48, has been generated in the tyrosine-free Y72F/Y108F mutant.[170] It is buried in a hydrophobic pocket, so it comes as no surprise that it has a g tensor that is more anisotropic ($g_z - g_x = 0.0015$ vs. 0.0013) than that of surface-exposed Trp108 (S. Stoll, unpublished 690 GHz spectra).

Solution. The Trp radicals in RNR and azurin are neutral Trp radicals, with the indole nitrogen deprotonated. The solution pK_a of the oxidized Trp radical is around 4.2, and could be tuned by proteins to stabilize either the deprotonated neutral or the protonated cation form of the radical at physiological pH. In solution, the Trp cation radical can be generated easily

at acidic pH[49] and has been studied using X-band EPR. However, there are currently no published experimental g tensors for protonated Trp radicals.

Haem enzymes. A protonated Trp radical at position 191 has unambiguously been identified in compound ES of cytochrome c peroxidase (CcP) using ENDOR on isotopically labelled samples,[171] but its g tensor is obscured by coupling to the $S = 1$ [Fe(IV) = O] haem. In a CcP-like mutant of horseradish peroxidase (F221W), a similar tryptophan radical (Trp221) could be detected,[172] although it is not clear whether it is protonated. A Trp radical as well as several Tyr radicals have been observed in *M. tuberculosis* haemoglobin O[173] treated with hydrogen peroxide. Hints of a tryptophan radical were also observed in cytochrome P450BMP.[141] It is commonly thought that these radicals are generated by oxidation through the porphyrin radical $P^{\bullet +}$ in compound I [Fe(IV) = O $P^{\bullet +}$].

Surface-exposed Trp radicals are the oxidizing agents in versatile peroxidases (VPs), fungal enzymes that are able to degrade lignin. The radicals in VP from two fungi have been studied: $Trp^{\bullet}$ in *Bjerkandera adusta*[174], possibly $Trp170^{\bullet}$, and $Trp164^{\bullet}$ in *P. eryngii*[175]. The two radicals have different side chain orientations[176], but the g tensors are identical to within 0.00005. By mutating Trp164 in *P. eryngii* VP to Tyr, the corresponding $Tyr^{\bullet}$ radical is observed[158], and enzymatic activity is significantly reduced. Recently, a lignin peroxidase (LiP) surface Trp site including the two amino acids from the Trp microenvironment were engineered into a peroxidase from *Coprinus cinereus*[177], yielding a triple-mutant enzyme with new lignin peroxidase activity. The same work also showed evidence of a radical on Trp121 in LiP.

Catalase-peroxidases (KatGs) are bifunctional haem-containing enzymes and have a remarkably high Trp content (22–25). Trp radicals were observed in several variants of KatG from *M. tuberculosis* (Trp321),[178] *Synechocystis* (Trp106),[179] and *Bulkholderia pseudomallei* (Trp330).[180]

A tryptophan radical has been kinetically resolved in cytochrome c oxidase (CcO) by microsecond freeze-hyperquenching and Q-band EPR,[181,182] with Trp272 identified as the radical site.

Others. Tryptophan radicals also occur in photolyases, where they have been observed coupled to flavin radicals (see section on flavin radicals).

5.3 Glycyl radicals

Glycyl radicals stand out among amino acid radicals, as the unpaired spin density is not delocalized over an aromatic ring π system on the side chain such as in Trp and Tyr, but located directly on the protein backbone mostly on a single atom, the α carbon. The g tensor of the glycyl radical was first estimated from low-field EPR studies of irradiated single crystals.[183,184]

Glycyl radical enzymes. Glycyl radicals are the catalytically active species in several enzymes that perform key metabolic steps in anaerobic bacteria.[185–187] The radicals in three of these enzymes, benzylsuccinate synthase,[188,189] pyruvate-formate lyase[190,191] and anaerobic class III ribonucleotide reductase,[119,192,193] have been characterized by high-field EPR.[70] Their g tensors are very similar, and the three g values lie so close

(span 0.0019–0.0023) that the g_x and g_y features still overlap at 285 GHz. Complete resolution is achieved only at 525 GHz.[70] From the g tensor it is clear that the glycyl radical is a π radical, with the spin density mostly concentrated in the $2p_z$ orbital of the α carbon in a trigonal-planar geometry. However, the g anisotropies are large compared to methyl radicals (e.g. in Maxixe-type beryl[194] $\Delta g = 0.00014$ at room temperature, but 0.00026 at $-150\,^{\circ}C$, and 0.0003 adsorbed on silica get at 77 K[195]). This indicates substantial spin density on neighbouring heteroatoms such as the two nearest carbonyl oxygens. Consistent with this finding, theoretical computations[196–199] estimate over 60% spin on C(α), but also indicate delocalization with up to about 10% spin each on the adjacent oxygens and nitrogens. These spin densities, as well as the g tensor, can be modulated by both intra- and intermolecular hydrogen bonds.

Others. A backbone radical has recently been observed in the [4Fe-4S] cluster protein ThiC[187] from *Salmonella enterica*, which is involved in thiamine biosynthesis. Its location is currently unknown, but Gly and Ala could be excluded based on the observed hyperfine structure in the X-band cw EPR spectrum.

5.4 Cysteine-derived sulphur radicals

A variety of sulphur-centred radicals[200] derived from cysteine have been observed in biological systems, including thiyl (R-S$^{\bullet}$), perthiyl (R-SS$^{\bullet}$), sulfinyl (R-SO$^{\bullet}$) and disulfide anion (R-S$^{\bullet}$S-R^{-}) radicals. Since sulphur has a large spin-orbit coupling constant, the g tensors of these radicals are very anisotropic and can easily be resolved at X-band. Unless their spectra overlap with several other radical species,[201] there is no need for high-field EPR. Nevertheless, for completeness a few aspects of cysteine-derived sulphur radicals will be mentioned here.

Radicals centred on the side chain of cysteine were first studied in the heydays of radiation research in UV-irradiated cysteine hydrochloride[202] and cystin dihydrochloride crystals[203] as well as in N-acteylcysteine.[204] The g_x values of thiyl radicals R-S$^{\bullet}$ range from 2.15 to 2.3[205] and vary substantially depending on the conformation of the radical and the number of hydrogen bonds to the sulphur. The unpaired spin resides in an almost pure 3p orbital of the sulphur atom, which is nearly degenerate with one of the lone pair orbitals.[206] This near-degeneracy causes the large g_x values and their exceptional sensitivity to the environment.

Protein-based thiyl radicals from cysteine and possibly methionine were observed in bovine serum albumin and R1 of *E. coli* RNR after low-temperature UV irradiation.[118,207,208] In all three classes of RNR, a cysteine thiyl radical is believed to function as the active residue that starts the turnover reaction by abstracting the 3′ hydrogen atom from the substrate. Despite strong indirect evidence, the thiyl radical could not be observed so far. However, a disulfide radical anion R-S$^{\bullet}$S-R^{-} could be detected in the active-site mutant α-E441Q of *E. coli* RNR[201]. It is located on C463 and C225 of the α subunit and was identified among several overlapping radicals by 140 GHz EPR with g values 2.023, 2.015 and 2.002. Quantum chemical

calculations are able to predict these values.[209] Originally, the radical was believed to be a cysteine thiyl radical.[210]

A cysteine-derived sulfinyl radical R-SO$^{\bullet}$ could be generated in the iron-oxygen reconstitution of a mouse RNR R2 protein mutant where the site of the tyrosyl radical was mutated to a phenylalanine (Y177F) and a cysteine (I263C) was inserted at the same distance to the di-iron centre as the Y177 radical in the wild type.[211] Its g tensor determined from X-band and 285 GHz spectra (2.0206, 2.0093, 2.0022) is typical for sulfinyl radicals.[212] A similar sulfinyl radical was observed in wild-type and mutant pyruvate-formate lyase inactivated by the exposure to dioxygen.[213,214] Sulfinyl radical therefore appear to form by oxygenation of thiyl radicals.

5.5 Cross-linked and modified amino acids

There exist a series of tyrosine-derived protein-based cofactors[215] that are redox active., e.g. in KatG, galactose oxidase, cytochrome c oxidase and copper amine oxidases.

Catalase-peroxidase (KatG) is a complex enzyme, not only due to its two enzymatic activities, but due to the variety of transient radicals that can be generated (see section on tyrosyl and tryptophan radicals). In the reaction of KatG from *M. tuberculosis*, *B. pseudomallei* and *Synechocystis* PCC6803 with excess hydrogen peroxide, radical signals with unusual g tensors are observed ($g_x = 2.00550$ and 2.00606, $g_y = 2.00344$, $g_z = 2.00186$).[216] Since the span (0.0036 and 0.0042) is narrower than that of tyrosyl radicals (0.005–0.007), but much wider than that of tryptophan radicals (0.0012–0.0013), the radical has been attributed to a ring-substituted Tyr, cross-linked with Met and Trp in the 3 and 5 positions (M255–Y229–W107 adduct).[217,218] The narrower g tensor compared to typical Tyr radicals is rationalized in terms of increased spin delocalization which reduces spin density on the tyrosine oxygen and thus the g_x value. In contrast, with peroxyacetic acid, typical Tyr and Trp radicals are observed and identified by their high-field EPR signature.[145,147,178,180,219]

The radical-copper enzyme galactose oxidase combines two one-electron acceptors, Cu(II) and a protein-based radical, in its active site. The radical is located on a 3*I*-(S-cysteinyl)tyrosine adduct (Tyr272-Cys228) that co-ordinates to the copper via the phenoxy oxygen of Tyr.[220,221] In copper-free apo-galactose oxidase, the radical on Cys-Tyr can be generated with high yield.[222] High-field EPR at 140 GHz reveals a nearly axial g tensor (2.00741, 2.00641, 2.00211) with a span typical for tyrosine radicals, but an unusually high g_y value.[223] Calculations have attributed the axiality of the g tensor to significant spin density on the sulphur.[223,224] The calculations also predict an in-plane angle of 12–38° between the g_x axis and the C–O axis of Tyr, but there are currently no experimental confirmations of this tilt. Recent detailed isotope labelling studies at X-band have probed the influence of the thioether linkage on the electronic ground state of the radical,[225] and a comparison to model compounds suggests the involvement of the phenoxy oxygen of Tyr in a hydrogen bond.[226] A stacking Trp has significant influence on the radical, lowering its redox potential and extending its lifetime.[227] A radical has also been identified in another radical-copper enzyme, glyoxal oxidase.[228]

In cytochrome c oxidase (CcO), the terminal enzyme in the respiratory chain that catalyzes the four-electron reduction of oxygen to water, a redox-active cross-linked tyrosine-histidine moiety (Tyr244-His240, with a covalent link between the ortho carbon of the phenoxy group and the ε nitrogen of histidine) is critical for activity.[101,221,229]

Copper amine oxidases[230] contain a post-translationally modified tyrosine, 2,4,5-trihydroxyphenylalanine quinone (topa quinone, TPQ), that is redox active and can exist in a paramagnetic semiquinone form.[231,232] Although it has been studied by pulse EPR methods,[233] the g tensor has apparently not been determined so far.

The tryptophan tryptophylquinone (TTQ) cofactor in methylamine dehydrogenase (MADH) is a quinone based on a covalent dimer of the indole rings from two tryptophans in the protein chain. The TTQ cofactor is post-translationally synthesized from the two tryptophan residues in a six-electron oxidation with the assistance of the di-heme enzyme MauG.[234] The TTQ semiquinone radical in MADH from *Paracoccus denitrificans* has been studied by low-field EPR.[235,236]

Modified amino acids have been site-specifically incorporated into ribonucleotide reductase using the suppressor tRNA/aminoacyl-tRNA synthetase methodology.[237] Replacement of various tyrosines with 3-aminotyrosine,[238,239] 3,4-dihydroxyphenylalanine (DOPA),[240,241] 3-nitrotyrosine[242] and various fluorinated tyrosines[243] allowed the trapping of kinetically competent radical intermediates along the radical propagation pathway from the tyrosyl radical in the cofactor subunit to the active site in the catalytic subunit. For the variants with incorporated 3-aminotyrosine, 180 GHz EPR spectra revealed a g tensor with g values of 2.00520, 2.00420 and 2.00220[239]. Compared to typical tyrosine radicals, the g_y is only minimally changed, but the g_x value is significantly reduced by the presence of 3-amino substituent. Additionally, a hydrogen bond to the phenoxy might be present. Fluorotyrosine has been incorporated in place of Y_Z in PS II to probe the coupling between proton and electron transfer,[244] but no high-field data are available.

6 Cofactor radicals

This section gives an overview of high-field EPR done on non-amino acid derived organic cofactor radicals that are predominantly noncovalently interacting with proteins. The main groups are flavins, chlorophylls, and benzo- and naphtha-quinones, but they also include a few less common ones such as pyrroloquinoline quinone and tetrahydrobiopterin.

6.1 Flavin radicals

The two flavin cofactors flavin adenine mononucleotide and flavin adenine dinucleotide (FMN and FAD) are among the most common redox-active organic cofactors in nature and can exist in one of three oxidation states: fully oxidized as shown in Fig. 6, one-electron reduced, and two-electron reduced. The paramagnetic one-electron reduced semiquinone form can occur as a neutral ($FlH^{\bullet}$) or as a deprotonated anionic ($Fl^{\bullet -}$) radical, depending on the protonation state of the ring nitrogen N(5).[245]

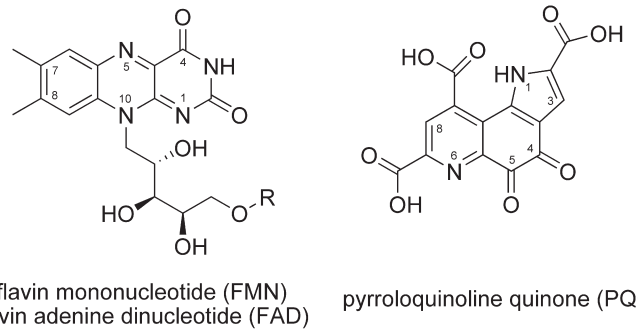

Fig. 6 Structure of the riboflavin part of the cofactors flavin adenine mononucleotide and flavin adenine dinucleotide (FMN and FAD, left), and of pyrroloquinoline quinone (PQQ, right). The oxidized quinone forms are shown, the semiquinone forms are obtained by one-electron reduction.

In the semiquinone, the unpaired electron is delocalized over the three rings of the dimethlyisoalloxazine core and is detectable via the hyperfine couplings of N(5) and N(10) as well as the protons at ring positions 5 and 6, on the 8-methyl group and on the CH_2 group attached to N(5).

The g tensors of neutral and anionic flavin radicals are quite distinct. Whereas g_x seems to be rather insensitive to the protonation state resulting in similar spans (0.0020–0.0022), their g_y values differ so that the skew of neutral radicals $FlH^{\bullet}$ is around 0.3, and the one of $Fl^{\bullet -}$ is about 0.2. Therefore, neutral and anionic flavins cluster in different regions in Fig. 3. For $Fl^{\bullet -}$, g_x and g_y are not visibly resolved at W-band, but using careful spectral fitting of second- and third-derivative spectra,[88,246] the g tensors could be extracted.

The g tensor of a flavin radical was first determined in deuterated systems.[29] The first high-field EPR spectrum (W-band) of a neutral flavin radical $FlH^{\bullet}$ in *E. coli* cyclobutane pyrimidine dimer (CPD) photolyase was reported in 1999,[247] and the g tensor was determined to be approximately axial. Later measurements of the same radical at 360 GHz gave more accurate g values and revealed a slight non-axiality.[248] The g tensor of $FlH^{\bullet}$ in *X. laevis* (6-4) photolyase as determined at W-band[249] and 360 GHz[250] is very similar to the one of the CPD photolyase radical. Neutral flavin radicals have also been characterized in two flavin-binding LOV domains of the blue-light receptor phototropin.[251]

The multi-flavin iron-sulphur membrane enzyme Na^+-translocating NADH:quinone oxidoreductase (Na^+-NQR) oxidizes NADH and transfers two electrons to ubiquinone, reducing it to ubiquinol. This redox reaction is coupled to the transfer of two sodium ions across the membrane. In Na^+-NQR from *Vibrio cholerae*, neutral and anionic flavin radical signals from FMN were observed,[88,252] and their g tensors were determined from W-band spectra. Recently, an additional riboflavin radical in Na^+-NQR has been reported.[253,254]

In the flavoenzyme glucose oxidase from *Aspergillus niger*, the photoreduced flavin radical is neutral at pH 5 and anionic at pH 10. Both were characterized at X- and W-band as well as 360 GHz.[255] Anionic flavin

radicals were identified by high-field EPR and ENDOR in monoamine oxidase (MAO) A and in D-amino acid oxidase.[48,246,256,257]

Most of the flavin cofactor radicals are noncovalently interacting with their respective proteins. Two of them are covalently bound to a cysteine residue of the protein: in MAO A to a cysteine through C(8α), and in phototropin LOV1 C57M-675 to the terminal carbon of a methionine through N(5). The latter is a neutral flavin and features a g tensor with principal values 2.00554, 2.00391, 2.00247 (span 0.0031, skew 0.53).[251] These values are significantly larger than in the noncovalent forms due to increased spin-orbit coupling resulting from the interaction of the methionine sulphur close to the N(5) with the electron spin density in the flavin π system. In MAO A, on the other hand, the flavin is covalently bound to a cysteine sulphur via C(8α). The skew of the g tensor does not deviate from other anionic flavins, but the span (0.0018) appears to be smaller due to an unusually high g_z value.

The protonation state of N(5) can also be determined by ENDOR[255] as demonstrated nicely by a recent extensive comparative ENDOR study.[258] In addition to the absence or presence of a broad ^{1}H signal due to H(5) with its large anisotropic hyperfine coupling, the hyperfine couplings of other protons are also characteristic of the protonation state. Even the X-band spectrum can show subtle differences between neutral and anionic radicals,[259–261] although hydrogen bonds of variable strength to N(5) or N(5)H can make an assignment based on these differences difficult.

Proteins from the photolyase/cryptochrome family contain a flavin cofactor and a conserved chain of three Trp to enable electron transfer from the protein surface to the flavin cofactor. The resulting flavin radicals have been studied by high-field EPR (see above), but intermittent tryptophan-flavin spin-polarized radical pairs have also been observed directly.[262,263]

In summary, the g tensor of flavins as obtained by high-field EPR, ideally above W-band, is a very clear reporter on the protonation state of N(5). It is also sensitive to covalent bonding, as known for Cys attachment at N(5) and C8α. From the currently available g tensor data, it appears that the effect of the protein environment on the flavin g tensor is small.

6.2 Chlorophylls

Chlorophylls (see Fig. 7) are the dominant pigment cofactors in the photosynthetic reaction centres of bacteria and plants, responsible for light absorption, energy transfer and charge separation. They are therefore of enormous interest. However, chlorophyll radicals are among the most challenging organic radicals in EPR, both experimentally and theoretically. The g tensor anisotropy is only 0.001 or even less (see Fig. 3). Consequently, very high fields and frequencies are needed to resolve the g tensor. For example, it takes frequencies beyond 100 GHz just to match the unresolved hyperfine linewidth of about 2 mT (see Fig. 2). In addition, the g tensor is hard to interpret and hyperfine couplings are difficult to assign. Chlorophylls are very large molecules, and the spin density is delocalized over the entire aromatic π system. No single atom (like the phenoxy oxygen in tyrosyl radicals) dominates the g tensor. Even though chlorophyll is apparently

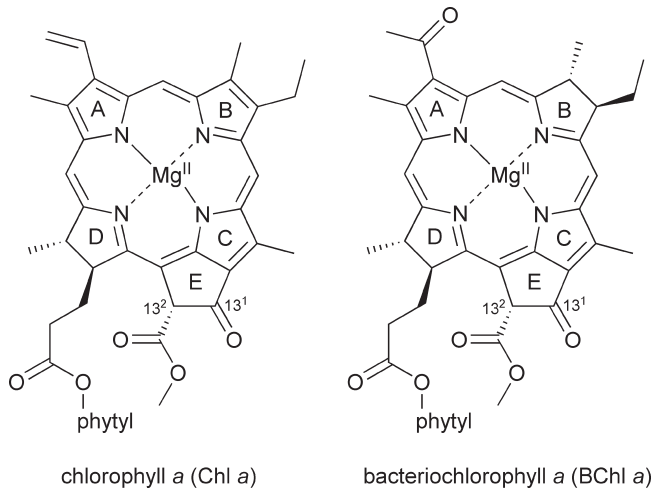

Fig. 7 Structure of chlorophyll *a* (Chl *a*, left) and bacteriochlorophyll *a* (BChl *a*, right). Chl *a′* and BChl *a′* are the 13^2 epimers of Chl *a* and BChl *a′*. The structures of pheophytin *a* and bacteriopheophytin *a* are obtained from the respective chlorophyll by removing the Mg^{2+} ion and protonating the pyrrole nitrogens on ring A and C.

a planar molecule, g tensor orientations have been found that do not align with this symmetry.

Chlorophylls have been studied in three systems: in photosystem I (PS I) and photosystem II (PS II) of plants and bacteria that perform oxygenic photosynthesis, and in photosynthetic reaction centres of non-oxygenic photosynthetic bacteria. High-field EPR studies that determined the g tensors and their molecular orientations of chlorophyll radicals started in the 1990s and stimulated the breakthrough in high-field EPR technology. There is a brief and excellent 2004 review on chlorophyll radicals[97] that summarizes the results and tabulates measured g tensors.

Solution. As a point of reference for the biological systems, chlorophyll radicals were generated in organic solvents and studied by high-field EPR. Due to solvent interactions and structural heterogeneity in frozen solution, the g values are distributed (g strain) and high-field spectra are broadened to an extent that makes it impossible to determine $\boldsymbol{g}$. However, in perdeuterated chlorophylls the lineshapes are partially narrowed so that the g tensors could be determined. The g values are (2.00329, 2.00375, 2.00220, span 0.00109) for $Chl_a^{\bullet+}$[264] and (2.00338, 2.00256, 2.00217, span 0.00121) for $BChl_a^{\bullet+}$,[265,266] both in CH_2Cl_2. Chl *a* radical ions have been investigated using semiempirical methods[264] and density functional theory,[267] with results in general agreement with experimental data.

Photosystem II. PS II contains many cofactors, among them at least 35 chlorophylls. A chlorophyll radical, together with a carotenoid radical, can be generated by illumination of PS II at low temperature. They appear to be part of a secondary electron transport chain that can donate an electron to the primary donor. Because the carotenoid spectrum overlaps the chlorophyll spectrum, experimental values of the g tensor of this so-called Chl *z* radical are not straightforward to obtain and are somewhat inconsistent.[97]

The anisotropy found ranges from 0.00091 to 0.00110,[34,40,83,268,269] but generally agrees with the one of monomeric chlorophyll in solution. Using samples with oriented membranes, it was found that the plane of the chlorophyll giving rise to this signal is approximately perpendicular to the membrane plane.[269] The distances between Chl *z* and other paramagnetic centres in PS II has been probed by pulsed EPR at 130 GHz.[270]

Bacterial reaction centres. The primary donor centre in reaction centres of purple bacteria,[271,272] denoted P_{865} in *Rhodobacter sphaeroides*, consists of a pair of bacteriochlorophylls BChl *a* (see Fig. 7). The g tensor of the cation radical $P_{865}^{\bullet+}$ was determined from EPR spectra at various frequencies, with a first estimate from Q-band[273] and more reliable values from high-field EPR at 95, 360 and 670 GHz.[40,42,43,52,66,107,265,274–277] In addition to *Rh. sphaeroides* wild type, the strain R-26 that lacks carotenoids has been used. From a pioneering 95 GHz single-crystal study,[42] it was found that the g_z axis in $P_{865}^{\bullet+}$ is tilted away from the plane normal of either BChl by about 22°. When the axial histidine ligand at position M202 is mutated to leucine (glutamate), the g anisotropy decreases (increases) as determined at 360 GHz.[276] The reader is referred to several detailed reviews[11,277,278] of the high-field EPR and ENDOR work on $P_{865}^{\bullet+}$.

The g tensor of the primary donor in its excited triplet state was determined from quinone-depleted RC[279] and gave 2.0037, 2.0028 and 2.0022. The anisotropy is larger than in the ground state.

In addition to the extensive studies done on *Rh. sphaeroides* $P_{865}^{\bullet+}$, g tensor data are available for the corresponding primary donor radicals $P_{960}^{\bullet+}$ from *Blastochloris* (formerly *Rhodopseudomonas*) *viridis*[68,280] and for $P_{870}^{\bullet+}$ from *Chloroflexus aurantiacus*.[275] In another study, BChl $c^{\bullet+}$ of chemically oxidized chlorosomes from two species of green bacteria[281] were investigated by high-field EPR and gave very narrow spectra, e.g. 2.00265, 2.00250 and 2.00210 (span 0.00045) for *C. aurantiacus* at 10 K and 330 GHz. The g anisotropy was found to decrease with increasing temperature, probably as a result of thermally driven electron exchange processes between several closely spaced bacteriochlorophylls.

Photosystem I. PS I coordinates many chlorophyll molecules. Two of them, one Chl *a* from the A side and one Chl *a′* from the B side (see Fig. 7) are in close proximity and form the primary donor P_{700}, similar to the bacterial reaction centres. Their planes are parallel, and they overlap partially. The two Chl are axially coordinated by histidines. Chl *a′* is hydrogen bonded to the protein via the keto oxygen and the methoxy group in ring E, whereas Chl *a* is not. Upon illumination in the presence of an electron acceptor, the one-electron oxidized cation radical $P_{700}^{\bullet+}$ is formed. $P_{700}^{\bullet+}$ has been extensively studied by EPR[97,282], and its g tensor has been determined from different organisms and under different conditions.[38–40,65,83,268,283] The g anisotropy is consistently found to be 0.0008–0.0009 and is the smallest known of all bioorganic radicals, smaller than that of chlorophyll *a* monomers (0.0011) and $P_{865}^{\bullet+}$ (0.0013). In fact, at 95–140 GHz, fully deuterated systems are needed to achieve the necessary resolution.[38–40,268,283] At 330 GHz one can determine the g tensor without deuteration,[65,83] although the g separation is still only partial. Surprisingly, the g values appear to be

temperature dependent[65]: Δg decreases from 0.00091 at 40K to 0.00081 at 200 K, mostly due to a decrease in g_x. Furthermore, single crystal studies at 95 GHz indicate an unexpected tilt of approximately 30° between the g_z axis and the chlorophyll plane normal.[39,283] This is contrary to what is expected from Stone theory in a planar aromatic system, where g_z is always perpendicular to the plane of the π system.

Neither the g_z axis tilt nor the surprisingly small g anisotropy are fully understood. Both seem to indicate increased delocalization over the chlorophyll pair. However, this is not consistent with ENDOR studies that suggest at most 15% of spin density on one of the chlorophylls.[282] Another possibility is that spin is localized predominantly on one monomer that is structurally distorted. This is supported by evidence from a 330 GHz EPR study on wild-type and mutants of *Chlamydomonas reinhardtii* PS I, where one or both of the histidines axially coordinating the chlorophyll Mg^{2+} ions are mutated to glutamine.[83] The mutation H656Q on the B side (at Chl *a*) increased the g anisotropy from 0.00084 to 0.00096 by decreasing the g_z value, whereas the analogous mutation H676Q on the A side (at Chl *a*') did not affect the g tensor. Another mutation on the A side, T739A, removes a hydrogen bonding partner to the 13^1 keto-oxygen, but has essentially no effect on the g tensor[83,284] From these data, a highly asymmetric spin distribution, mostly localized on the B-side Chl *a*, and a deviation of this Chl from planarity due to the axial ligand seems likely.

It would be interesting to determine how the g tensor orientation is affected by these mutations. It might be that the tilt and the small anisotropy are due to the stacking between the two monomers. The effect of the degree of stacking on a potential delocalized electronic structure and the g tensor has been explored by density functional theory using small aromatic hydrocarbon models,[285] with unclear implications for Chl*a*-Chl*a*′ in PS I. In summary, despite a substantial amount of excellent EPR data, the electronic structure of the $P_{700}^{\bullet+}$ cation radical and the origin of its magnetic parameters are currently not fully understood.

Pheophytin. An intermediate electron acceptor in the electron transfer chain of photosynthetic reaction centres, (bacterio)pheophytin *a*, corresponds to demetallated (bacterio)chlorophyll *a*. Its radical anion state has been trapped and studied by high-field EPR at 285 GHz.[110,286] The radical anions of pheophytin in spinach PS II ($Pheo^{\bullet-}$) and bacteriopheophytin in bacterial reaction centers from *Bc. viridis* ($BPheo^{\bullet-}$) feature very narrow g tensors with g_x values of 2.00424 and 2.00437, respectively.[110] By mutating a glutamine that functions as a hydrogen bonding partner to the ring E carbonyl oxygen of one of the pheophytins in *C. reinhardtii* PS II, clear shifts in the g_x value of the radical could be observed.[286] Replacing the glutamine by leucine results in an increase from 2.00420 to 2.00440, which is consistent with the loss of the hydrogen bond and confirms that there is significant spin density on the ring E carbonyl oxygen.

6.3 Benzo- and naphthoquinones

Benzo- and naphthoquinones constitute a large group of cofactors. The most important naturally occurring ones are shown in Fig. 8. Their

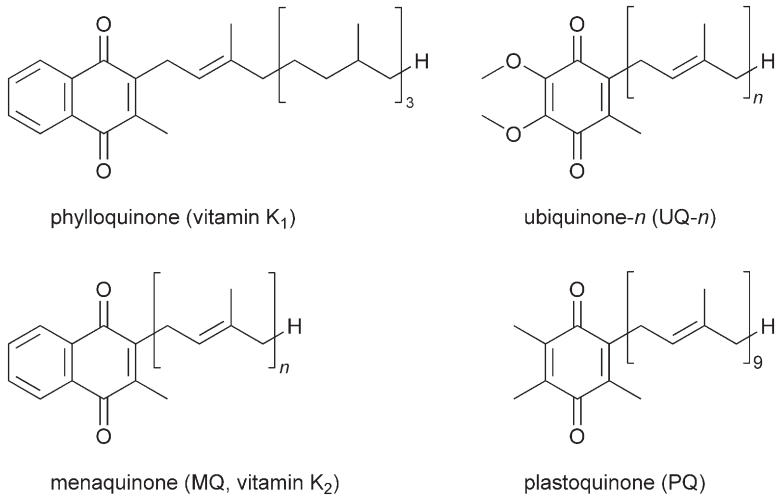

Fig. 8 Structures of several naturally occurring naphtho- and benzoquinones. After addition of one electron to the dione ring π system, the associated radical anions are formed.

common structural motif is a 1,4-quinone group, which can be reduced by one electron to the paramagnetic anionic semiquinone, and by a second electron to the 1,4-diol form. The semiquinones have been studied intensely by high-field EPR since the early 1990s, and at least four dozen g tensors both in enzyme systems and *in vitro* can be found in the literature. Several reviews discuss EPR of semiquinone cofactors in photosynthesis.[287,288]

Despite the different chemical structures, the g tensors of benzo- and naphthoquinones are not clearly different. Benzoquinones tend to have g tensors with somewhat larger spans and larger skews, but environmental effects cause a lot of overlap between the two groups, so that they are clustered together in the plot of Fig. 8. Hydrogen bonds, such as provided by the solvent in alcoholic solutions,[283,289], decrease the g anisotropy and the skew. The g anisotropies are large enough ($\Delta g \approx 0.004$) that g tensors can be determined from Q-band spectra of deuterated quinones in deuterated solvents.[36]

Various natural and model benzo- and naphthoquinones have been examined in protic and aprotic solvents,[32,36,62,283,289–292] including naphtho-, dimethylnaphtho-, benzo-, dimethylbenzo- and duroquinone as well as vitamin K_3. In addition, extensive quantum chemical calculations on semiquinones have been performed.[36,293–297] Generally, the agreement between experiment and theory is excellent.

Bacterial reaction centres. Quinones are the final electron acceptors in bacterial photosynthetic reaction centres. A recent book collects reviews on many aspects of purple phototrophic bacteria.[272] More specifically, high-field EPR on bacterial reaction centres was summarized recently.[277] The early seminal work on quinones in bacterial reaction centres is collected in a 1999 review,[298] and further EPR work is discussed in another review by Lubitz.[288]

The acceptor quinones Q_A and Q_B in bacterial reaction centres may be ubiquinones (e.g. *Rh. sphaeroides*) or menaquinones (e.g. in *Bc. viridis*), see

Fig. 8. In addition to the quinone head, only the first two isoprene units of the tail are interacting tightly with the protein. The signal from the acceptor quinones in bacterial reaction centres is resolvable only if the nearby Fe^{2+} site is substituted by Zn^{2+}.

Two landmark studies[32,289] first determined the g tensor of $Q_A^{\bullet -}$, with values of 2.0065, 2.0053 and 2.0022, with an anisotropy/span of 0.0043. Burghaus[289] compared it to model quinones in solution using W band EPR, and Isaacson[299] used single-crystal Q-band EPR on deuterated ubiquinone-10 in the Q_A site to determine both the g tensor of $Q_A^{\bullet -}$ and its orientation with respect to the crystal. By comparison to the crystal structure with the quinone Q_A, the orientation of the cofactor was found to remain essentially unchanged upon reduction. A high-time resolution and high-field EPR study of the radical pair consisting of $Q_A^{\bullet -}$ and the primary donor $P_{865}^{\bullet +}$ found that the headgroup of Q_A is undergoing a 60° rotational reorientation upon reduction.[300]

Isaacson[299] also measured the g tensor of $Q_B^{\bullet -}$, observing a g_x of 2.0062, slightly smaller compared to $Q_A^{\bullet -}$. In a recent 360 GHz study, Schnegg[277] was able to observe and resolve the signals of two quinones simultaneously, one being $Q_A^{\bullet -}$ and the second one $Q_B^{\bullet -}$ based on a comparison to the known g value.

It is also possible to generate a $Q_A^{\bullet -}Q_B^{\bullet -}$ biradical state, using several methods.[301] From high-field EPR at 35, 95 and 326 GHz,[301,302] the exchange coupling constant between the two radicals could be determined.

Photosystem I. In PS I, a phylloquinone (see Fig. 8) in a site denoted as A_1 acts as electron acceptor. Its semiquinone form $A_1^{\bullet -}$ can be observed either in an isolated form generated by photoaccumulation or as part of the radical pair $P_{700}^{\bullet +}A^{\bullet -}$ with the primary donor. The g tensor of $A_1^{\bullet -}$ has been determined from both forms.[39,283,292,303,304] Its anisotropy is in the range 0.00390–0.00405, which is much larger than the one for the same radical in alcoholic solutions (0.00337–0.00363, depending on the alcohol),[36,62,283,289,290] but similar when aprotic solvents are used (e.g. 0.00403 in DME-MTHF[283,291]). This is consistent with a predominantly hydrophobic binding pocket in PS I with less hydrogen bonding compared to alcoholic solutions. A similar g tensor behaviour is observed when naphthoquinone or duroquinone are substituted into the A_1 site.[303]

The phylloquinone radical and its binding site were recently characterized with pulse Q-band EPR and ENDOR,[305] and a single H-bond was found to govern the electronic structure of the quinone. When a tryptophan that is π stacked with the quinone is mutated to Phe, the g principal values do not change noticeably, indicating that the electronic structure is not strongly disturbed.[306]

In the unusual chlorophyll *d*-containing PS I of the cyanobacterium *Acaryochloris marina*, Santabarbara[307] identified a quinone as secondary electron acceptor.

Photosystem II. PS II contains two plastoquinones (PQ-9, see Fig. 8), Q_A and Q_B, that act as sequential electron acceptors. Q_A is a one-electron acceptor and hands the electron on to Q_B, which accepts two electrons and dissociates after double protonation. As in bacterial reaction centres, both

quinones are coupled to a nearby Fe^{2+} ($S = 2$) ion. The semiquinone form of the plastoquinone in the Q_A site can be generated by chemical reduction in iron-depleted PS II. Compared to the semiquinone radicals in bacterial reaction centres and PS I, $Q_A^{\bullet -}$ has received little attention from high-field EPR. The g tensor was first estimated from Q-band EPR spectra[308] and later determined accurately from its 285 GHz spectrum,[110] yielding an anisotropy of 0.00446. Compared to $Q_A^{\bullet -}$ in Zn-substituted bacterial reaction centres[32], the anisotropy is similar, but the g_y value is lower. In the same study, the orientation of the semiquinone could be determined from oriented samples and turned out to be comparable to bacterial reaction centres.

Other systems. Even though quinones in photosynthetic centres have received most attention, quinones occurs in other systems as well. One example is nitrate reductase A from *E. coli*.[309] The radical in the quinol oxidation site in the subunit NarI has been studied by ESEEM[310,311], but no high-field data are available.

Very recently, the g tensor of menasemiquinone in *Bacillus subtilis* cytochrome aa_3-600 menaquinol oxidase was determined from Q-band EPR,[312] giving the principal values 2.00642, 2.00540 and 2.00228 (span 0.00414).

A quinone acts as the terminal electron acceptor in Na^+-NQR, but no high-field data are available for this system.

Cytochrome bo_3 (ubiquinol oxidase, QOX) from *E. coli*[313,314] features a ubisemiquinone radical. It has been modelled using DFT by Kaczprak,[296] and a model with hydrogen bonds to both oxygens has been proposed.

The spectrum of the semiquinone anion form of ubiquinone-6 in cytochrome bc_1 ($Q_i^{\bullet -}$) was observed recently, and a typical g tensor was obtained from the analysis of the Q-band spectrum.[315] Also, ESEEM studies have probed the hydrogen bonds in the binding site.[316]

6.4 Other cofactors

Pyrroloquinoline quinine. Pyrroloquinoline quinone (PQQ, see Fig. 6) is a noncovalent cofactor in several alcohol dehydrogenases. One of them, quinoprotein ethanol dehydrogenase (QEDH), converts ethanol to acetaldehyde. During the catalytic cycle, the oxidized PQQ cofactor accepts a hydride from the substrate to give the quinol form $PQQH_2$ which is subsequently reoxidized by two single-electron transfers[317] via the intermediate semiquinone $PQQ^{\bullet -}$. An unusual disulfide bond between two neighbouring cysteines adjacent to the cofactor is essential for reoxidation under physiological conditions.[318] The semiquinone form has been studied by EPR in QEDH from *P. aeruginosa*.[317,319–321] Interestingly, a double cysteine-alanine mutation does not affect the EPR spectrum, as the mutant exhibits g values practically identical to the wild type (2.00575, 2.00512, 2.00209 vs. 2.00571, 2.00413, 2.00207, respectively).[319] Upon substrate binding, all three g values decrease slightly[320], indicating structural or polarity changes close to the cofactor. The EPR work of QEDH has recently been reviewed.[322]

Quinone cofactors occur in other alcohol dehydrogenases, and EPR signals from the semiquinone forms have been observed, e.g. PQQ in

methanol dehydrogenase (MDH),[323] soluble glucose dehydrogenase (sGDH)[324] and quinohemoprotein alcohol dehydrogenase (ADH)[325] as well as TTQ in methylamine dehydrogenase (MADH, see section on modified amino acids).[235,236] Membrane-bound glucose dehydrogenase (mGDH) features a ubisemiquinone cofactor that assists the electron transfer from PQQ to the external electron acceptor.[326,327] There are no published high-field EPR data on the radicals in these enzymes.

Carotenoid. PS II also features a signal from a carotenoid cation radical ($Car^{\bullet +}$) that can be generated by illumination at low temperatures.[328] Its g principal values, (2.00322, 2.00252 and 2.00211) in spinach[269] and (2.00335, 2.00251, 2.00227) in *Synechococcus lividus*,[34] are similar in anisotropy and consistent with the anisotropy found for the radical cation of the carotenoid cantaxanthin in a form adsorbed on silica-alumina as studied by 95–670 GHz EPR ($g_{||} = 2.0032$, $g_{\perp} = 2.0023$).[67] The small anisotropy is explained by the delocalization of the spin density over at least 14 carbons and the absence of spin density on the carbonyl oxygens. A recent study on neutral carotenoid radicals on a molecular sieve[329] led to a proposal of an electron transfer pathway from Car with an adjacent proton acceptor to $P_{680}^{\bullet +}$.

Tetrahydrobiopterin. The tetrahydrobiopterin cofactor in the flavo-haem enzyme nitric oxide synthase serves as a reversible electron donor to the haem active site during the catalytic cycle. The transient paramagnetic one-electron oxidized state can be trapped,[330,331] and EPR spectra recorded at above 400 GHz yielded a g tensor with principal values 2.00430, 2.00353 and 2.00210.[332] Together with ENDOR spectra and theoretical calculations, it could be determined that the cofactor does not undergo deprotonation upon oxidation, which is different from its behaviour in solution and unusual compared to other redox-active cofactors. The flavin radical from nitric oxide synthase has been observed as well,[333] but no high-field data are available.

5′-Deoxyadenosyl. A radical that is famously missing in this review, although it is very important in biology, is 5′-deoxyadenosyl (5′-dA). It is the active agent of many vitamin B_{12} dependent enzymes and of enzymes in the large radical S-adenosyl-L-methionine (SAM) superfamily.[334] In B_{12}-dependent reactions, the radical is generated by homolytic cleavage of the Co–C bond in adenosylcobalamin. Radical SAM enzymes generate 5′-dA via reductive cleavage of S-adenosyl-L-methionine by a 4Fe-4S cluster. The radical then performs various chemical tasks such as hydrogen abstraction from a substrate. For EPR spectroscopists, 5′-dA is too shortlived to allow trapping during enzymatic turnover. Only an allylic analogue could be trapped.[335] No high-field data are available. Using photoinduced bond cleavage of adenosylcobalamin in solution, 5′-dA could be observed by Fourier transform EPR.[336]

Others. In anaerobic organisms, pyruvate:ferredoxin oxidoreductase (PFOR) decarboxylates pyruvate and depends on a thiamine diphosphate (ThDP) cofactor. During turnover, the EPR spectrum of a radical intermediate is observed. From ENDOR studies,[337] it was proposed that the unpaired electron resides on a hydroxylethylidene-ThDP intermediate, which has been shown to have a markedly non-planar ring structure.[338]

7 Substrate radicals

Obviously, enzyme substrates in nature are very diverse, and so are substrate radicals. In this section we present those that have been studied in detail with high-field EPR, but also mention some others of current interest.

RNR. The same active-site mutant α-E441Q of *E. coli* RNR that yields a disulfide radical in the active site as discussed above subsequently produces a radical on the substrate, cytidine diphosphate (CDP). The unpaired electron was originally proposed to be located on the 4′ position of the sugar ring with a keto group at the 3′ position.[201] This assignment was based on the measured g principal values (2.0072, 2.0061 and 2.0021) and the hyperfine structure. A recent study[75] employed substrates isotope labelled with ^{2}H, ^{13}C, or ^{15}N together with ENDOR and high-field EPR to examine this assignment. Surprisingly, the radical was found to be a 2′,3′-semidione, the one-electron reduced form of a 2′,3′-diketone, with the unpaired electron delocalized over two carbons and two oxygens. The radical is very likely not on the normal catalytic pathway.

The class II RNR from *Lactobacillus leichmannii* is inactivated by the substrate analogue 2′,2′-difluoro-2′-deoxycytidine-5′-triphosphate, and a radical intermediate can be trapped by freeze-quenching. Using high-field ENDOR at 130 GHz, a sugar-based 3′-keto, 2′-oxoallylic radical[339] similar to that observed in the α-E441Q mutant of *E. coli* RNR was proposed.[340]

PcyA. The enzyme phycocyanobilin:ferredoxin oxidoreductase (PcyA) converts the tetrapyrrole biliverdin to phycocyanobilin (PCB), an important chromophore for cyanobacterial light harvesting and for bacterial and plant light sensing. The four-electron reduction proceeds via single-electron transfers from an external reductant to the substrate and includes two paramagnetic intermediate substrate states. The first of these was recently trapped and characterized by high-field EPR at 130 GHz (single crystals) and 416 GHz (frozen solutions).[47] The g tensor (2.00359, 2.00341, 2.00218) is almost axial and almost as narrow as the ones from chlorophyll radicals. The narrowness is due to the extended delocalization of the unpaired electron spin over the four pyrrole rings. Based on DFT modelling, the small anisotropy and the near-axiality of the g tensor appears to be a result of the protonation of both carbonyl oxygens.

Others. Recently, a radical intermediate has been detected during the reaction of methyl-coenzyme M reductase (MCR) from *Methanothermobacter marburgensis* with bromoethanesulfonate. The exact nature of the radical is not currently known, although tyrosyl has been ruled out by high-field EPR and ENDOR combined with isotope substitution.[341] MCR has been the target of a series of advanced EPR studies.[342,343]

Dph2 is an iron-sulphur enzyme involved in diphthamide biosynthesis. In Dph2 from *Pyrococcus horikoshii*, it was recently shown that an intermittent 3-amino-3-carboxypropyl radical is generated by the unusual $C_{\gamma,Met}$–S bond cleavage of the cofactor S-adenosyl-L-methionine.[344] This radical then crosslinks with a histidine on the substrate, protein elongation factor 2 (EF2).

Another intriguing radical reaction occurs in the biosynthetic pathway of phosphinothricin, a natural compound that is synthetically produced and used as a herbicide. The mononuclear non-haem iron enzyme hydroxyethylphosphonate dioxygenase converts 2-hydroxyethylphosphonate to hydroxymethylphosphonate, removing the CH_2 group from a P–CH_2–C motif, and a substrate-radical intermediate is currently proposed.[345]

One of the enzymes of porphyrin biosynthesis, coproporphyrinogen III oxidase HemN, performs oxidative decarboxylations of two propionate side chains of the substrate. During turnover of *E. coli* HemN, a coproporphyrinogenyl III substrate radical has been observed and studied by X-band cw EPR in combination with selective isotope labeling.[35] The unpaired spin is delocalized over one pyrrole ring and an attached carbon. No high-field EPR data are available yet.

The multi-copper oxidase enzyme laccase can be used in conjunction with redox mediators to oxidize large organic substrates such as lignin. When laccases from two white-rot fungi were used together with the redox mediators violuric acid (VIO) and 2,2′-azino-bis-(3-ethylbenzothiazoline-6-sulfonic acid) (ABTS), mediator-based oxidized neutral and cation radicals were detected and characterized at 9, 35 and 244 GHz.[346]

An amino acid radical that is not protein-based is the lysine substrate radical in lysine-2,3-aminomutase. It has been studied by ENDOR spectroscopy.[347]

8 Other radicals

Free radicals. There exists a whole gamut of biological ''free'' radicals that are not located on or associated with enzymes, but nonetheless are of utmost biological importance. These radicals are not within the scope of this overview, which concentrates on ''bound'' radicals. They are discussed in a recent review in this series.[348] This group includes reactive oxygen species (ROS) such as the superoxide and hydroxyl radicals $O_2^{\bullet -}$ and $HO^{\bullet}$ which can cause serious damage in cells, and the more benign reactive nitrogen species (RNS) such as the important physiological messenger nitric oxide $NO^{\bullet}$. Also, many small-molecule antioxidants/reductants yield free radicals of which ascorbyl, the one-electron oxidation product of ascorbate, is an example.

Free radicals can also occur in an *in vitro* environment. Ascorbyl has recently been trapped in a reaction mixture of cytochrome c oxidase with oxygen and ascorbate as reductant.[349] Its g tensor, as determined by 130 GHz EPR, is almost axial (2.0068, 2.0066, 2.0023). When dithionite is used as a reductant instead of ascorbate, the $SO_2^{\bullet -}$ anion radical anion was observed, with g values 2.0089, 2.0052, 2.0017.[349] Therefore, care has to be exercised if these reductants are used in reactions where other radicals are generated. Ascorbate and dithionite can contribute to the spectra and obscure other radical signals.

Humic acids. Humic acids are major components of humic substances in humus, peat and coal and consist of a network of interlinked phenolic motifs with carboxy side groups and 1,2-quinone functions. Radicals have been detected in natural humic acids and were examined in several recent

high-field EPR studies.[98,350,351] One of them[98] used 285 GHz EPR to look at naturally occurring humic acids and found two different types of indigenous stable radicals, one dominant at acidic pH (2.0032, 2.0023) and the other in basic solutions (2.0057, 2.0055, 2.0023). The g tensor of the low-pH radical indicates extended delocalization, whereas the high-pH form appears to have significant spin density on oxygens or nitrogens, with possible semiquinone character. Another study[351] used the semiquinone form of 3,4-dihydroxybenzoic acid as a model, determined the g tensor from 400 GHz spectra and successfully predicted it using DFT methods. The principal values of the nearly axial g tensor (2.00620, 2.00570, 2.00257) are comparable to those of $PQQ^{\bullet -}$, a structurally similar 1,2-semiquinone. Gallic acid, 3,4,5-trihydroxybenzoic acid, is another model for humic acids.[352]

Radiation-generated radicals. Many radicals can be generated by γ, X-ray or UV irradiation of biological materials such as proteins, amino acids, carbohydrates and DNA. The radicals resulting from γ irradiating DNA are mostly located on the nucleobases, and it has been shown that cytosine and thymine are the sites of reduction, and guanine is the site where holes locate. EPR in the context of DNA radiation chemistry has been expertly summarized in several reviews in this series, most recently in 2008.[353,354] Here we briefly mention only the guanine radical, where some interesting EPR results have appeared. Using X-band EPR, isotope labelling and DFT calculations, the structure of the guanine radical cation $G^{\bullet +}$ and its singly and doubly deprotonated forms could be characterized.[355] In multi-G oligomers, the hole localization site could be determined using deuterium-labelled G selectively inserted into specific positions.[356] It would be interesting to use high-field EPR to study the effect of nucleobase structure and protonation state on the g tensor of this type of radical.

Irradiation of sugars also generates radicals that are being studied by EPR. The g tensors have been derived both at X-band[357,358] and at W-band and above.[359,360]

EPR at 285 GHz has been used in a study to identify radicals in irradiated drugs.[361] The g tensors of the radicals induced in the β blockers atenolol and esmolol were determined.

9 Summary

The field of bioorganic high-field EPR is very active and diverse. For many bioorganic radicals, abundant sets of g tensor data are available. Some, like tryptophans, have not been studied as extensively as others. In many cases, clear correlations between the g tensor and structural properties are observed. Through these, high-field EPR can yield direct structural insight. Importantly, the g tensor yields information on protonation states and hydrogen bonds, two structural aspects that are not accessible from X-ray crystallography. The correlations between g tensors and structural properties are well characterized and modelled by quantum mechanical calculations that can predict g tensors fairly accurately when the radical is embedded in its immediate surrounding environment.

The future will certainly see progress in all directions, but a few developments would be especially welcome. On the experimental side, a general

and portable solution of the experimental problem of accurately measuring absolute g factors at high field would be desirable. On the theoretical side, one area that remains largely unexplored but would have enormous cross-disciplinary benefits is the question how g tensors and electronic properties such as redox potentials relate to each other.

References

1 J. Z. Pedersen and A. Finazzi-Agrò, *FEBS Lett*., 1993, **325**, 53–58.
2 J. A. Stubbe and W. A. van der Donk, *Chem. Rev*., 1998, **98**, 705–762.
3 P. A. Frey, *Annu. Rev. Biochem*., 2001, **70**, 121–148.
4 A. Savitsky, A. A. Dubinskii, M. Plato, Y. A. Grishin, H. Zimmermann and K. Möbius, *J. Phys. Chem. B*, 2008, **112**, 9079–9090.
5 Z. Zhang, M. R. Fleissner, D. S. Tipikin, Z. Liang, J. M. Moscicki, K. A. Earle, W. L. Hubbell and J. H. Freed, *J. Phys. Chem. B*., 2010, **114**, 5503–5521.
6 K. K. Andersson and A.-L. Barra, *Spectrochim. Acta A*, 2002, **58**, 1101–1112.
7 A.-L. Barra, A. Gräslund and K. K. Andersson, in *Very High Frequency (VHF) ESR/EPR*, eds. O. Grindberg and L. J. Berliner, Kluwer Academic/Plenum Publishers, New York, edition 2004, Vol. **22**, pp. 145–163.
8 M. Bennati and T. F. Prisner, *Rep. Prog. Phys*., 2005, **68**, 411–448.
9 G. Jeschke, *Biochim. Biophys. Acta*, 2005, **1707**, 91–102.
10 A. Savitsky and K. Möbius, *Photosynth. Res*., 2009, **102**, 311–333.
11 K. Möbius and A. Savitsky, *High-Field EPR Spectroscopy on Proteins and their Model Systems: Characterization of Transient Paramagnetic States*, Royal Society of Chemistry, Cambridge, UK, 2009.
12 A. Carrington and A. D. McLachlan, *Introduction to Magnetic Resonance*, Harper and Row, New York, 1967.
13 N. M. Atherton, *Principles of Electron Spin Resonance*, Ellis Horwood, Chichester, 1993.
14 D. Hanneke, S. Fogwell and G. Gabrielse, *Phys. Rev. Lett*., 2008, **100**, 120801.
15 J. T. Törring, S. Un, M. Knüpling, M. Plato and K. Möbius, *J. Chem. Phys*., 1997, **107**, 3905–3913.
16 L. F. Chibotaru, A. Ceulemans and H. Bolvin, *Phys. Rev. Lett*., 2008, **101**, 033003.
17 S. Stoll and A. Schweiger, *J. Magn. Reson*., 2006, **178**, 42–55.
18 M. H. L. Pryce, *Proc. Phys. Soc. A*, 1950, **63**, 25–29.
19 A. J. Stone, *Proc. Roy. Soc. London*, 1963, **271**, 424–434.
20 A. J. Stone, *Mol. Phys*., 1963, **6**, 509–515.
21 R. Angstl, *Chem. Phys*., 1989, **132**, 435–442.
22 M. Gerloch, *Orbitals, Terms and States*, Wiley, Chichester, 1986.
23 J. A. Weil and J. R. Bolton, *Electron Paramagnetic Resonance. Elementary Theory and Practical Applications*, Wiley, Hoboken, 2007.
24 M. Blume and R. E. Watson, *Proc. Roy. Soc. Lond. A*, 1963, **271**, 565–578.
25 C. J. Pickard and F. Mauri, *Phys. Rev. Lett*., 2002, **88**, 086403.
26 A. Soncini, *J. Chem. Theory Comput*., 2007, **3**, 2243–2257.
27 S. Koseki, M. W. Schmidt and M. S. Gordon, *J. Phys. Chem*., 1992, **96**, 10768–10772.
28 F. Neese, *J. Chem. Phys*., 2005, **122**, 034107.
29 J. R. Norris and H. L. Crespi, *Chem. Phys. Lett*., 1972, **16**, 542–547.
30 A. van der Est, R. Bittl, E. C. Abresch, W. Lubitz and D. Stehlik, *Chem. Phys. Lett*., 1993, **212**, 561–568.
31 A.-L. Tsai, L. C. Hsi, R. J. Kulmacz, G. Palmer and W. L. Smith, *J. Biol. Chem*., 1994, **269**, 5085–5091.

32 R. A. Isaacson, F. Lendzian, E. C. Abresch, W. Lubitz and G. Feher, *Biophys. J.*, 1995, **69**, 311–322.
33 F. Lendzian, M. Sahlin, F. MacMillan, R. Bittl, R. Fiege, S. Pötsch, B.-M. Sjöberg, A. Gräslund, W. Lubitz and G. Lassmann, *J. Am. Chem. Soc.*, 1996, **118**, 8111–8120.
34 K. V. Lakshmi, M. J. Reifler, G. W. Brudvig, O. G. Poluektov, A. M. Wagner and M. C. Thurnauer, *J. Phys. Chem. B.*, 2000, **104**, 10445–10448.
35 G. Layer, A. J. Pierik, M. Trost, S. E. J. Rigby, H. K. Leech, K. Grage, D. Breckau, I. Astner, L. Jänsch, P. Heathcote, M. J. Warren, D. W. Heinz and D. Jahn, *J. Biol. Chem.*, 2006, **281**, 15727–15734.
36 B. Epel, J. Niklas, S. Sinnecker, H. Zimmermann and W. Lubitz, *J. Phys. Chem. B.*, 2006, **110**, 11549–11560.
37 T. Maly, J. Bryant, D. Ruben and R. G. Griffin, *J. Magn. Reson.*, 2006, **183**, 303–307.
38 T. F. Prisner, A. E. McDermott, S. Un, J. R. Norris, M. C. Thurnauer and R. G. Griffin, *Proc. Natl. Acad. Sci. U.S.A.*, 1993, **90**, 9485–9488.
39 S. G. Zech, W. Hofbauer, A. Kamlowski, P. Fromme, D. Stehlik, W. Lubitz and R. Bittl, *J. Phys. Chem. B.*, 2000, **104**, 9728–9739.
40 O. G. Poluektov, L. M. Utschig, S. L. Schlesselman, K. V. Lakshmi, G. W. Brudvig, G. Kothe and M. C. Thurnauer, *J. Phys. Chem. B*, 2002, **106**, 8911–8916.
41 A. van Roggen, L. van Roggen and W. Gordy, *Phys. Rev.*, 1957, **105**, 50–55.
42 R. Klette, J. T. Törring, M. Plato, K. Möbius, B. Bonigk and W. Lubitz, *J. Phys. Chem.*, 1993, **97**, 2015–2020.
43 M. Huber and J. T. Törring, *Chem. Phys.*, 1995, **194**, 379–385.
44 W. Hofbauer, A. Zouni, R. Bittl, J. Kern, P. Orth, F. Lendzian, P. Fromme, H. T. Witt and W. Lubitz, *Proc. Natl. Acad. Sci. U.S.A.*, 2001, **98**, 6623–6628.
45 M. Högbom, M. Galander, M. Andersson, M. Kolberg, W. Hofbauer, G. Lassmann, P. Nordlund and F. Lendzian, *Proc. Natl. Acad. Sci. U.S.A.*, 2003, **100**, 3209–3214.
46 M. Galander, M. Uppsten, U. Uhlin and F. Lendzian, *J. Biol. Chem.*, 2006, **281**, 31743–31752.
47 S. Stoll, A. Gunn, M. Brynda, W. Sughrue, A. C. Kohler, A. Ozarowski, A. J. Fisher, J. C. Lagarias and R. D. Britt, *J. Am. Chem. Soc.*, 2009, **131**, 1986–1995.
48 V. J. DeRose, J. C. G. Woo, W. P. Hawe, B. M. Hoffman, R. B. Silverman and K. Yelekci, *Biochemistry*, 1996, **35**, 11085–11091.
49 H. D. Connor, B. E. Sturgeon, C. Mottley, H. J. Sipe, Jr. and R. P. Mason, *J. Am. Chem. Soc.*, 2008, **130**, 6381–6387.
50 E. J. Reijerse, *Appl. Magn. Reson.*, 2010, **37**, 795–818.
51 G. M. Smith and P. C. Riedi, in *Electron Paramagnetic Resonance, A Specialist Periodical Report*, eds. N. M. Atherton, M. J. Davies, B. C. Gilbert and K. A. McLauchlan, The Royal Society of Chemistry, London, edition, 2000, Vol. **17**, pp. 164-204.
52 R. J. Hulsebosch, I. V. Borovykh, S. V. Paschenko, P. Gast and A. J. Hoff, *J. Phys. Chem. B*, 1999, **103**, 6815–6823.
53 H. C. Yeh, G. J. Gerfen, J. S. Wang, A. L. Tsai and L. H. Wang, *Biochemistry*, 2009, **48**, 917–928.
54 G. J. Gerfen, B. F. Bellew, S. Un, J. M. Bollinger, J. Stubbe, R. G. Griffin and D. J. Singel, *J. Am. Chem. Soc.*, 1993, **115**, 6420–6421.
55 L. R. Becerra, G. J. Gerfen, B. F. Bellew, J. A. Bryant, D. A. Hall, S. J. Inati, R. T. Weber, S. Un, T. F. Prisner, A. E. McDermott, K. W. Fishbein, K. E.

Kreischer, R. J. Temkin, D. J. Singel and R. G. Griffin, *J. Magn. Reson. A*, 1995, **117**, 28–40.
56 C. T. Farrar, G. J. Gerfen, R. G. Griffin, D. A. Force and R. D. Britt, *J. Phys. Chem. B*, 1997, **101**, 6634–6641.
57 M. Rohrer, O. Brügmann, B. Kinzer and T. F. Prisner, *Appl. Magn. Reson.*, 2001, **21**, 257–274.
58 E. Reijerse, P. P. Schmidt, G. Klihm and W. Lubitz, *Appl. Magn. Reson.*, 2007, **31**, 611–626.
59 F. Muller, M. A. Hopkins, N. Coron, M. Grynberg, L. C. Brunel and G. Martinez, *Rev. Sci. Instrum.*, 1989, **60**, 3681–3684.
60 K. A. Earle, B. Dzikovski, W. Hofbauer, J. K. Moscicki and J. H. Freed, *Magn. Reson. Chem.*, 2005, **43**, 256–266.
61 H. Blok, J. A. J. M. Disselhorst, S. B. Orlinskii and J. Schmidt, *J. Magn. Reson.*, 2004, **166**, 92–99.
62 S. Un, P. Dorlet and A. W. Rutherford, *Appl. Magn. Reson.*, 2001, **21**, 341–361.
63 M. R. Fuchs, T. F. Prisner and K. Möbius, *Rev. Sci. Instrum.*, 1999, **70**, 3681–3683.
64 Y. A. Grishin, M. R. Fuchs, A. Schnegg, A. A. Dubinskii, B. S. Dumesh, F. S. Rusin, V. L. Bratman and K. Möbius, *Rev. Sci. Instrum.*, 2004, **75**, 2926–2936.
65 P. J. Bratt, M. Rohrer, J. Krzystek, M. C. W. Evans, L.-C. Brunel and A. Angerhofer, *J. Phys. Chem. B*, 1997, **101**, 9686–9689.
66 P. J. Bratt, E. Ringus, A. K. Hassan, J. van Tol, A. L. Maniero, L.-C. Brunel, M. Rohrer, C. Bubenzer-Hange, H. Scheer and A. Angerhofer, *J. Phys. Chem. B*, 1999, **103**, 10973–10982.
67 T. A. Konovalova, J. Krzystek, P. J. Bratt, J. van Tol, L.-C. Brunel and L. D. Kispert, *J. Phys. Chem. B*, 1999, **103**, 5782–5786.
68 P. J. Bratt, P. Heathcote, A. Hassan, J. van Tol, L.-C. Brunel, J. Schrier and A. Angerhofer, *Chem. Phys.*, 2003, **294**, 277–284.
69 S. A. Zvyagin, J. Krzystek, P. H. M. van Loosdrecht, G. Dhalenne and A. Revcolevschi, *Physica B*, 2004, **346–247**, 1–5.
70 C. Duboc-Toia, A. K. Hassan, E. Mulliez, S. Ollagnier-de Choudens, M. Fontecave, C. Leutwein and J. Heider, *J. Am. Chem. Soc.*, 2003, **125**, 38–39.
71 A. K. Hassan, L. A. Pardi, J. Krzystek, A. Sienkiewicz, P. Goy, M. Rohrer and L.-C. Brunel, *J. Magn. Reson.*, 2000, **142**, 300–312.
72 P. A. S. Cruickshank, D. R. Bolton, D. A. Robertson, R. I. Hunter, R. J. Wylde and G. M. Smith, *Rev. Sci. Instrum.*, 2009, **80**, 103102.
73 P. J. Mohr, B. N. Taylor and D. B. Newell, *Rev. Mod. Phys.*, 2008, **80**, 633–730.
74 S. Un, J. Bryant and R. G. Griffin, *J. Magn. Reson. A*, 1993, **101**, 92–94.
75 H. Zipse, E. Artin, S. Wnuk, G. J. S. Lohman, D. Martino, R. G. Griffin, S. Kacprzak, M. Kaupp, B. M. Hoffman, M. Bennati, J. Stubbe and N. Lees, *J. Am. Chem. Soc.*, 2009, **131**, 200–211.
76 A. Stesmans and G. Van Gorp, *Rev. Sci. Instrum.*, 1989, **60**, 2949–2952.
77 A. Stesmans and G. Van Gorp, *Phys. Lett. A*, 1989, **139**, 95–98.
78 W. Low, *Phys. Rev.*, 1957, **105**, 793–800.
79 M. A. Ondar, O. Y. Grinberg, A. A. Dubinski, A. F. Shestakov and Y. S. Lebedev, *Khim. Fiz.*, 1983, **2**, 54.
80 O. Burghaus, M. Rohrer, T. Götzinger, M. Plato and K. Möbius, *Meas. Sci. Technol.*, 1992, **3**, 765–774.
81 G. Feher, *Phys. Rev.*, 1959, **114**, 1219–1244.
82 A. Stesmans and G. De Vos, *Phys. Rev. B*, 1986, **34**, 6499–6502.

83 A. Petrenko, A. L. Maniero, J. van Tol, F. MacMillan, Y. J. Li, L. C. Brunel and K. Redding, *Biochemistry*, 2004, **43**, 1781–1786.
84 J. Krzystek, A. Sienkiewicz, L. A. Pardi and L.-C. Brunel, *J. Magn. Reson.*, 1997, **125**, 207–211.
85 N. D. Yordanov, *Appl. Magn. Reson.*, 1996, **10**, 339–350.
86 S. V. Kolaczkowski, J. T. Cardin and D. E. Budil, *Appl. Magn. Reson.*, 1999, **16**, 293–298.
87 S. A. Goldman, G. V. Bruno, C. F. Polnaszek and J. H. Freed, *J. Chem. Phys.*, 1972, **56**, 716–735.
88 B. Barquera, J. E. Morgan, D. Lukoyanov, C. P. Scholes, R. B. Gennis and M. J. Nilges, *J. Am. Chem. Soc.*, 2003, **125**, 265–275.
89 K. Möbius, *Z. Naturforsch. A*, 1965, **20**, 1102–1116.
90 B. Cage, A. Weekley, L.-C. Brunel and N. S. Dalal, *Anal. Chem.*, 1999, **71**, 1951–1957.
91 B. Gross, H. Dilger, R. Scheuermann, M. Paech and E. Roduner, *J. Phys. Chem. A*, 2001, **105**, 10012–10017.
92 K.-P. Dinse, in *Electron Paramagnetic Resonance, A Specialist Periodical Report*, eds. B. C. Gilbert, M. J. Davies and K. A. McLauchlan, The Royal Society of Chemistry, Cambridge, edition, 2000, Vol. **17**, pp. 78-108.
93 S. Stoll, A. Ozarowski, R. D. Britt and A. Angerhofer, *J. Magn. Reson.*, 2010, **207**, 158–163.
94 F. G. Herring and P. S. Phillips, *J. Magn. Reson.*, 1984, **59**, 489–496.
95 R. K. Harris, E. D. Becker, S. M. Cabral De Menezes, P. Granger, R. E. Hoffman and K. W. Zilm, *Solid State Nucl. Magn. Reson.*, 2008, **33**, 41–56.
96 D. A. Svistunenko and C. E. Cooper, *Biophys. J*, 2004, **87**, 582–595.
97 A. Angerhofer, *Biol. Magn. Reson.*, 2004, **22**, 495–505.
98 K. C. Christoforidis, S. Un and Y. Deligiannakis, *J. Phys. Chem. A*, 2007, **111**, 11860–11866.
99 Y. S. Lebedev, in *Modern Pulsed and Continuous-Wave Electron Spin Resonance*, eds. L. Kevan and M. K. Bowman, John Wiley, New York, , 1990, pp. 365–404.
100 R. P. Pesavento and W. A. van der Donk, *Adv. Protein Chem.*, 2001, **58**, 317–385.
101 C. W. Hoganson and C. Tommos, *Biochim. Biophys. Acta*, 2004, **1655**, 116–122.
102 S. Y. Reece, J. J. Woodward and M. A. Marletta, *Biochemistry*, 2009, **48**, 5483–5491.
103 S. Un, M. Atta, M. Fontecave and A. W. Rutherford, *J. Am. Chem. Soc.*, 1995, **117**, 10713–10719.
104 A. W. Rutherford, A. Boussac and P. Faller, *Biochim. Biophys. Acta*, 2004, **1655**, 222–230.
105 M. Brok, F. C. R. Ebscamp and A. J. Hoff, *Biochim. Biophys. Acta*, 1985, **809**, 421–428.
106 C. W. Hoganson and G. T. Babcock, *Biochemistry*, 1992, **31**, 11874–11980.
107 V. I. Gulin, S. A. Dikanov, Y. D. Tsvetkov, R. G. Evelo and A. J. Hoff, *Pure Appl. Chem.*, 1992, **64**, 903.
108 S. Un, L.-C. Brunel, T. M. Brill, J.-L. Zimmermann and A. W. Rutherford, *Proc. Natl. Acad. Sci. U.S.A.*, 1994, **91**, 5262–5266.
109 S. Un, X.-S. Tang and B. A. Diner, *Biochemistry*, 1996, **35**, 679–684.
110 P. Dorlet, A. W. Rutherford and S. Un, *Biochemistry*, 2000, **39**, 7826–7834.
111 P. Faller, C. Coussias, A. W. Rutherford and S. Un, *Proc. Nat. Acad. Sci. U.S.A.*, 2003, **100**, 8732–8735.
112 H. Mino and A. Kawamori, *Photosynth. Res.*, 2008, **98**, 151–157.

113 S. Un, A. Boussac and M. Sugiura, *Biochemistry*, 2007, **46**, 3138–3150.
114 N. Ioannidis, G. Zahariou and V. Petrouleas, *Biochemistry*, 2008, **47**, 6292–6300.
115 L. Benisvy, R. Bittl, E. Bothe, C. D. Garner, J. McMaster, S. Ross, C. Teutloff and F. Neese, *Angew. Chem. Int. Ed.*, 2005, **44**, 5314–5317.
116 M. Brynda and R. D. Britt, *Res. Chem. Intermed.*, 2007, **33**, 863–883.
117 G. F. Moore, M. Hambourger, M. Gervaldo, O. G. Poluektov, T. Rajh, D. Gust, T. A. Moore and A. L. Moore, *J. Am. Chem. Soc.*, 2008, **130**, 10466–10467.
118 F. Lendzian, *Biochim. Biophys. Acta*, 2005, **1707**, 67–90.
119 N. Nordlund and P. Reichard, *Annu. Rev. Biochem.*, 2006, **75**, 681–706.
120 P. J. van Dam, J.-P. Willems, P. P. Schmidt, S. Pötsch, A.-L. Barra, W. R. Hagen, B. M. Hoffman, K. K. Andersson and A. Gräslund, *J. Am. Chem. Soc.*, 1998, **120**, 5080–5085.
121 E. Elleingand, C. Gerez, S. Un, M. Knüpling, G. Lu, J. Salem, H. Rubin, S. Sauge-Merle, J.-P. Laulhère and M. Fontecave, *Eur. J. Biochem.*, 1998, **258**, 485–490.
122 G. Bleifuss, M. Kolberg, S. Pötsch, W. Hofbauer, R. Bittl, W. Lubitz, A. Gräslund, G. Lassmann and F. Lendzian, *Biochemistry*, 2001, **40**, 15362–15368.
123 P. Allard, A.-L. Barra, K. K. Andersson, P. P. Schmidt, M. Atta and A. Gräslund, *J. Am. Chem. Soc.*, 1996, **118**, 895–896.
124 P. P. Schmidt, K. K. Andersson, A.-L. Barra, L. Thelander and A. Gräslund, *J. Biol. Chem.*, 1996, **271**, 23615–23618.
125 A. Liu, A.-L. Barra, H. Rubin, G. Lu and A. Gräslund, *J. Am. Chem. Soc.*, 2000, **122**, 1974–1978.
126 G. Bar, M. Bennati, H.-H. T. Nguyen, J. Ge, J. Stubbe and R. G. Griffin, *J. Am. Chem. Soc.*, 2001, **123**, 3569–3576.
127 S. Sauge-Merle, J.-P. Laulhère, J. Covès, L. le Pape, S. Ménage and M. Fontecave, *J. Biol. Inorg. Chem.*, 1997, **2**, 586–594.
128 E. Torrents, M. Sahlin, D. Biglino, A. Gräslund and B.-M. Sjöberg, *Proc. Natl. Acad. Sci. U.S.A.*, 2005, **102**, 17946–17951.
129 K. K. Andersson, P. P. Schmidt, B. Katterle, K. R. Strand, A. E. Palmer, S.-K. Lee, E. I. Solomon, A. Gräslund and A.-L. Barra, *J. Biol. Inorg. Chem.*, 2003, **8**, 235–247.
130 A. Liu, S. Pötsch, A. Davydov, A.-L. Barra, H. Rubin and A. Gräslund, *Biochemistry*, 1998, **37**, 16369–16377.
131 J. M. Bollinger, Jr., W. Jiang, M. T. Green and C. Krebs, *Curr. Opin. Struct. Biol.*, 2008, **18**, 650–657.
132 J. A. Cotruvo and J. Stubbe, *Biochemistry*, 2010, **49**, 1297–1309.
133 B. Abbouni, W. Oehlmann, P. Stolle, A. J. Pierik and G. Auling, *Free Radical Res.*, 2009, **43**, 943–950.
134 N. Cox, H. Ogata, P. Stolle, E. Reijerse, G. Auling and W. Lubitz, *J. Am. Chem. Soc.*, 2010, **132**, 11197–11213.
135 M. Engström, F. Himo, A. Gräslund, B. Minaev, O. Vahtras and H. Ågren, *J. Phys. Chem. A.*, 2000, **104**, 5149–5153.
136 S. Un, C. Gerez, E. Elleingand and M. Fontecave, *J. Am. Chem. Soc.*, 2001, **123**, 3048–3054.
137 M. Lucarini, V. Mugnaini, G. F. Pedulli and M. Guerra, *J. Am. Chem. Soc.*, 2003, **125**, 8318–8329.
138 A. Ivancich, T. A. Mattioli and S. Un, *J. Am. Chem. Soc.*, 1999, **121**, 5743–5753.
139 V. Schünemann, A. X. Trautwein, C. Jung and J. Terner, *Hyperfine Interact.*, 2002, **141/142**, 279–284.

140 V. Schünemann, F. Lendzian, C. Jung, J. Contzen, A.-L. Barra, S. G. Sligar and A. X. Trautwein, *J. Biol. Chem.*, 2004, **279**, 10919–10930.
141 C. Jung, V. Schünemann, F. Lendzian, A. X. Trautwein, J. Contzen, M. Galander, L. H. Böttger, M. Richter and A.-L. Barra, *Biol. Chem.*, 2005, **386**, 1043–1053.
142 J. C. Wilson, G. Wu, A.-L. Tsai and G. J. Gerfen, *J. Am. Chem. Soc.*, 2005, **127**, 1618–1619.
143 C. E. Rogge, W. Liu, R. J. Kulmacz and A.-L. Tsai, *J. Inorg. Biochem.*, 2009, **103**, 912–922.
144 P. Dorlet, S. A. Seibold, G. T. Babcock, G. J. Gerfen, W. L. Smith, A.-L. Tsai and S. Un, *Biochemistry*, 2002, **41**, 6107–6114.
145 S. Chouchane, S. Girotto, S. Yu and R. S. Magliozzo, *J. Biol. Chem.*, 2002, **277**, 42633–42638.
146 X. Zhao, S. Girotto, S. Yu and R. S. Magliozzo, *J. Biol. Chem.*, 2004, **279**, 7606–7612.
147 K. Ranguelova, S. Girotto, G. J. Gerfen, S. Yu, J. Suarez, L. Metlitsky and R. S. Magliozzo, *J. Biol. Chem.*, 2007, **282**, 6255–6264.
148 A. Ivancich, H. M. Jouve and J. Gaillard, *J. Am. Chem. Soc.*, 1996, **118**, 12852–12853.
149 A. Ivancich, H. M. Jouve, B. Sartor and J. Gaillard, *Biochemistry*, 1997, **36**, 9356–9364.
150 A. J. Fielding, R. Singh, B. Boscolo, P. C. Loewen, E. M. Ghibaudi and A. Ivancich, *Biochemistry*, 2008, **47**, 9781–9792.
151 A. Ivancich, P. Dorlet, D. B. Goddin and S. Un, *J. Am. Chem. Soc.*, 2001, **123**, 5050–5058.
152 A. Ivancich, G. Mazza and A. Desbois, *Biochemistry*, 2001, **40**, 6860–6866.
153 V. P. Miller, D. B. Goddin, A. E. Friedman, C. Hartmann and P. R. Ortiz de Montellano, *J. Biol. Chem.*, 1995, **270**, 18413–18419.
154 J. Feducia, R. Dumarieh, L. B. G. Gilvey, T. Smirnova, S. Franzen and R. A. Ghilardi, *Biochemistry*, 2009, **48**, 995–1005.
155 J. D'Antonio, E. L. D'Antonio, M. K. Thompson, E. F. Bowden, S. Franzen, T. Smirnova and R. A. Ghilardi, *Biochemistry*, 2010, **49**, 6600–6616.
156 F. MacMillan, A. Kannt, J. Behr, T. Prisner and H. Michel, *Biochemistry*, 1999, **38**, 9179–9184.
157 D. A. Proshlyakov, M. A. Pressler, C. DeMaso, J. F. Leykam, D. L. DeWitt and G. T. Babcock, *Science*, 2000, **290**, 1588–1591.
158 F. J. Ruiz-Dueñas, R. Pogni, M. Morales, S. Giansanti, M. J. Mate, A. Romero, M. J. Martínez, R. Basosi and A. T. Martínez, *J. Biol. Chem.*, 2009, **284**, 7986–7994.
159 C. Bernini, A. Sinicropi, R. Basosi and R. Pogni, *Appl. Magn. Reson.*, 2010, **37**, 279–288.
160 D. A. Svistunenko, J. Dunne, M. Fryer, P. Nicholls, B. J. Reeder, M. T. Wilson, M. G. Bigotti, F. Cutruzzolà and C. E. Cooper, *Biophys. J*, 2002, **83**, 2845–2855.
161 C. H. Chang, D. Svedružić, A. Ozarowski, L. Walker, G. Yeagle, R. D. Britt, A. Angerhofer and N. G. J. Richards, *J. Biol. Chem.*, 2004, **279**, 52840–52849.
162 T. Conrads, C. Hemann and R. Hille, *Biochemistry*, 1998, **37**, 7787–7791.
163 S. Weber, C. W. M. Kay, H. Mögling, K. Möbius, K. Hitomi and T. Todo, *Proc. Natl. Acad. Sci. U.S.A.*, 2002, **99**, 1319–1322.
164 C. Aubert, K. Brettel, P. Mathis, A. P. M. Eker and A. Boussac, *J. Am. Chem. Soc.*, 1999, **121**, 8659–8660.
165 E. L. Fasanella and W. Gordy, *Proc. Natl. Acad. Sci. U.S.A.*, 1969, **62**, 299–304.

166 H. C. Box, E. E. Budzinski and H. G. Freund, *J. Chem. Phys.*, 1974, **61**, 2222–2226.
167 A. L. Maniero, V. Chis, A. Zoleo, M. Brustolon and A. Mezzetti, *J. Phys. Chem. B*, 2008, **112**, 3812–3820.
168 A. Mezzetti, A. L. Maniero, M. Brustolon, G. Giacometti and L. C. Brunel, *J. Phys. Chem. A*, 1999, **103**, 9636–9643.
169 J. E. Miller, C. Grădinaru, B. R. Crane, A. J. Di Bilio, W. A. Wehbi, S. Un, J. R. Winkler and H. B. Gray, *J. Am. Chem. Soc.*, 2003, **125**, 14220–14221.
170 H. S. Shafaat, B. S. Leigh, M. J. Tauber and J. E. Kim, *J. Am. Chem. Soc.*, 2010, **132**, 9030–9039.
171 J. E. Huyett, P. E. Doan, R. Gurbiel, A. L. P. Houseman, M. Sivaraja, D. B. Goddin and B. M. Hoffman, *J. Am. Chem. Soc.*, 1995, **117**, 9033–9041.
172 A. Morimoto, M. Tanaka, S. Takahashi, K. Ishimori, H. Hori and I. Morishima, *J. Biol. Chem.*, 1998, **273**, 14753–14760.
173 H. Ouellet, K. Ranguelova, M. LaBarre, J. B. Wittenberg, B. A. Wittenberg, R. S. Magliozzo and M. Guertin, *J. Biol. Chem.*, 2007, **282**, 7491–7503.
174 R. Pogni, M. C. Baratto, S. Giansanti, C. Teutloff, J. Verdin, B. Valderrama, F. Lendzian, W. Lubitz, R. Vazquez-Duhalt and R. Basosi, *Biochemistry*, 2005, **44**, 4267–4274.
175 R. Pogni, M. C. Baratto, C. Teutloff, S. Giansanti, F. J. Ruiz-Dueñas, T. Choinowski, K. Piontek, A. T. Martínez, F. Lendzian and R. Basosi, *J. Biol. Chem.*, 2006, **281**, 9517–9526.
176 R. Pogni, C. Teutloff, F. Lendzian and R. Basosi, *Appl. Magn. Reson.*, 2007, **31**, 509–526.
177 A. T. Smith, W. A. Doyle, P. Dorlet and A. Ivancich, *Proc. Nat. Acad. Sci. U.S.A.*, 2009, **106**, 16084–16089.
178 R. Singh, J. Switala, P. C. Loewen and A. Ivancich, *J. Am. Chem. Soc.*, 2007, **129**, 15954–15963.
179 C. Jakopitsch, C. Obinger, S. Un and A. Ivancich, *J. Inorg. Biochem.*, 2006, **100**, 1091–1099.
180 J. Colin, B. Wiseman, J. Switala, P. C. Loewen and A. Ivancich, *J. Am. Chem. Soc.*, 2009, **131**, 8557–8563.
181 F. G. M. Wiertz, O.-M. H. Richter, A. V. Cherepanov, F. MacMillan, B. Ludwig and S. de Vries, *FEBS Lett.*, 2004, **575**, 127–130.
182 F. G. M. Wiertz, O.-M. H. Richter, B. Ludwig and S. de Vries, *J. Biol. Chem.*, 2007, **282**, 31580–31591.
183 I. Miyagawa, Y. Kurita and W. Gordy, *J. Chem. Phys.*, 1960, **33**, 1599–1603.
184 G. Saxebøl, T. B. Melø and T. Henriksen, *Radiat. Res.*, 1972, **51**, 31–44.
185 T. Selmer, A. J. Pierik and J. Heider, *Biol. Chem.*, 2005, **386**, 981–988.
186 W. Buckel and B. T. Golding, *Annu. Rev. Microbiol.*, 2006, **60**, 27–49.
187 N. C. Martinez-Gomez, R. R. Poyner, S. O. Mansoorabadi, G. H. Reed and D. M. Downs, *Biochemistry*, 2009, **48**, 217–219.
188 C. J. Krieger, W. Roseboom, S. P. J. Albracht and A. M. Spormann, *J. Biol. Chem.*, 2001, **276**, 12924–12927.
189 L. Li, D. P. Patterson, C. C. Fox, B. Lin, P. W. Coschigano and E. N. G. Marsh, *Biochemistry*, 2009, **48**, 1284–1292.
190 J. M. Buis and J. B. Broderick, *Arch. Biochem. Biophys.*, 2005, **433**, 288–296.
191 J. L. Vey, J. Yang, M. Li, W. E. Broderick, J. B. Broderick and C. L. Drennan, *Proc. Natl. Acad. Sci. U.S.A.*, 2008, **105**, 16137–16141.
192 X. Sun, S. Ollagnier, P. P. Schmidt, M. Atta, E. Mulliez, L. Lepape, R. Eliasson, A. Gräslund, M. Fontecave, P. Reichard and B.-M. Sjöberg, *J. Biol. Chem.*, 1996, **271**, 6827–6831.

193 M. Fontecave, E. Mulliez and D. T. Logan, *Prog. Nucleic Acid Res. Mol. Biol.*, 2002, **72**, 95–127.
194 L. O. Andersson, *Phys. Chem. Minerals*, 2008, **35**, 505–520.
195 T. Shiga and A. Lund, *J. Phys. Chem.*, 1973, **77**, 453–455.
196 I. Ciofini, C. Adamo and V. Barone, *J. Chem. Phys.*, 2004, **121**, 6710–6718.
197 S. Un, *Magn. Reson. Chem.*, 2005, **43**, S229–S236.
198 S. Kacprzak, R. Reviakine and M. Kaupp, *J. Phys. Chem. B*, 2007, **111**, 820–831.
199 S. Kacprzak, R. Reviakine and M. Kaupp, *J. Phys. Chem. B*, 2007, **111**, 811–819.
200 Z. B. Alfassi, ed., *S-Centered Radicals*, Wiley, New York, 1999.
201 C. C. Lawrence, M. Bennati, H. V. Obias, G. Bar, R. G. Griffin and J. Stubbe, *Proc. Natl. Acad. Sci. U.S.A.*, 1999, **96**, 8979–8984.
202 H. C. Box, H. G. Freund and E. E. Budzinski, *J. Chem. Phys.*, 1966, **45**, 809–811.
203 K. Akasaka, S.-I. Ohnishi, T. Suita and I. Nitta, *J. Chem. Phys.*, 1964, **40**, 3110–3116.
204 K. Matsuki, J. H. Hadley, W. H. Nelson and C.-Y. Yang, *J. Magn. Reson. A*, 1993, **103**, 196–202.
205 D. Nelson and M. C. R. Symons, *Chem. Phys. Lett.*, 1975, **36**, 340–341.
206 M. van Gastel, W. Lubitz, G. Lassmann and F. Neese, *J. Am. Chem. Soc.*, 2004, **126**, 2237–2246.
207 M. Kolberg, G. Bleifuss, A. Gräslund, B.-M. Sjöberg, W. Lubitz, F. Lendzian and G. Lassmann, *Arch. Biochem. Biophys.*, 2002, **403**, 141–144.
208 G. Lassmann, M. Kolberg, G. Bleifuss, A. Gräslund, B.-M. Sjöberg and W. Lubitz, *Phys. Chem. Chem. Phys.*, 2003, **5**, 2442–2453.
209 M. Engström, O. Vahtras and H. Ågren, *Chem. Phys. Lett.*, 2000, **328**, 483–491.
210 A. L. Perrson, M. Sahlin and B.-M. Sjöberg, *J. Biol. Chem.*, 1998, **273**, 31016–31020.
211 A. Adrait, M. Öhrström, A.-L. Barra, L. Thelander and A. Gräslund, *Biochemistry*, 2002, **41**, 6510–6516.
212 S. G. Swarts, D. Becker, S. DeBolt and M. D. Sevilla, *J. Phys. Chem.*, 1989, **93**, 155–161.
213 S. G. Reddy, K. K. Wong, C. V. Parast, J. Peisach, R. S. Magliozzo and J. W. Kozarich, *Biochemistry*, 1998, **37**, 558–563.
214 W. Zhang, K. K. Wong, R. S. Magliozzo and J. W. Kozarich, *Biochemistry*, 2001, **40**, 4123–4130.
215 M. Mure, *Acc. Chem. Res.*, 2004, **37**, 131–139.
216 J. Suarez, K. Ranguelova, A. A. Jarzecki, J. Manzerova, V. Krymov, X. Zhao, S. Yu, L. Metlitsky, G. J. Gerfen and R. S. Magliozzo, *J. Biol. Chem.*, 2009, **284**, 7017–7029.
217 X. Zhao, S. Yu, K. Ranguelova, J. Suarez, L. Metlitsky, J. P. M. Schelvis and R. S. Magliozzo, *J. Biol. Chem.*, 2009, **284**, 7030–7037.
218 X. Zhao, J. Suarez, A. Khajo, S. Yu, L. Metlitsky and R. S. Magliozzo, *J. Am. Chem. Soc.*, 2010, **132**, 8268–8269.
219 J. Colin, C. Jakopitsch, C. Obinger and A. Ivancich, *Appl. Magn. Reson.*, 2010, **37**, 267–277.
220 J. W. Whittaker, *Chem. Rev.*, 2003, **103**, 2347–2364.
221 M. S. Rogers and D. M. Dooley, *Curr. Opin. Chem. Biol.*, 2003, **7**, 189–196.
222 G. T. Babcock, M. K. El-Deeb, P. O. Sandusky, M. M. Whittaker and J. W. Whittaker, *J. Am. Chem. Soc.*, 1992, **114**.

223 G. J. Gerfen, B. F. Bellew, R. G. Griffin, D. J. Singel, C. A. Ekberg and J. W. Witthaker, *J. Phys. Chem.*, 1996, **100**, 16739–16748.
224 M. Kaupp, T. Gress, R. Reviakine, O. L. Malkina and V. G. Malkin, *J. Phys. Chem. B.*, 2003, **107**, 331–337.
225 Y.-K. Lee, W. M. Whittaker and J. W. Whittaker, *Biochemistry*, 2008, **47**, 6637–6649.
226 L. Benisvy, D. Hammond, D. J. Parker, E. S. Davies, C. D. Garner, J. McMaster, C. Wilson, F. Neese, E. Bothe, R. Bittl and C. Teutloff, *J. Inorg. Biochem.*, 2007, **101**, 1859–1864.
227 M. S. Rogers, E. M. Tyler, N. Akyumani, C. R. Kurtis, R. K. Spooner, S. E. Deacon, S. Tamber, S. J. Firbank, K. Mahmoud, P. F. Knowles, S. E. V. Phillips, M. J. McPherson and D. M. Dooley, *Biochemistry*, 2007, **46**, 4606–4618.
228 M. M. Whittaker, P. J. Kersten, N. Nakamura, J. Sanders-Loehr, E. S. Schweizer and J. W. Whittaker, *J. Biol. Chem.*, 1996, **271**, 681–687.
229 M. Voiescu, Y. El Khoury, D. Martel, M. Heinrich and P. Hellwig, *J. Phys. Chem. B*, 2009, **113**, 13429–13436.
230 H. C. Dawkes and S. E. V. Phillips, *Curr. Opin. Struct. Biol.*, 2001, **11**, 666–673.
231 R. Matsuzaki, S. Suzuki, K. Yamaguchi, T. Fukui and K. Tanizawa, *Biochemistry*, 1995, **34**, 4524–4530.
232 S. Hirota, T. Iwamoto, K. Tanizawa, O. Adachi and O. Yamauchi, *Biochemistry*, 1999, **38**, 14256–14263.
233 K. Warncke, G. T. Babcock, D. M. Dooley, M. A. McGuirl and J. McCracken, *J. Am. Chem. Soc.*, 1994, **116**, 4028–4037.
234 L. M. R. Jensen, R. Sanishvili, V. L. Davidson and C. M. Wilmot, *Science*, 2010, **327**, 1392–1394.
235 V. Singh, Z. Zhu, V. L. Davidson and J. McCracken, *J. Am. Chem. Soc.*, 2000, **122**, 931–938.
236 D. Ferrari, M. Di Valentin, D. Carbonera, A. Merli, Z.-w. Chen, F. S. Mathews, V. L. Davidson and G. L. Rossi, *J. Biol. Inorg. Chem.*, 2004, **9**, 231–237.
237 T. S. Young and P. G. Schultz, *J. Biol. Chem.*, 2010, **285**, 11039–11044.
238 M. R. Seyedsayamdost, J. Xie, C. T. Y. Chan, P. G. Schultz and J. Stubbe, *J. Am. Chem. Soc.*, 2007, **129**, 15060–15071.
239 M. R. Seyedsayamdost, T. Argirević, E. C. Minnihan, J. Stubbe and M. Bennati, *J. Am. Chem. Soc.*, 2009, **131**, 15729–15738.
240 M. R. Seyedsayamdost and J. Stubbe, *J. Am. Chem. Soc.*, 2006, **128**, 2522–2523.
241 M. R. Seyedsayamdost and J. Stubbe, *J. Am. Chem. Soc.*, 2007, **129**, 2226–2227.
242 K. Yokoyama, U. Uhlin and J. Stubbe, *J. Am. Chem. Soc.*, 2010, **132**, 8385–8397.
243 M. R. Seyedsayamdost, C. S. Yee, S. Y. Reece, D. G. Nocera and J. Stubbe, *J. Am. Chem. Soc.*, 2006, **128**, 1562–1568.
244 F. Rappaport, A. Boussac, D. A. Force, J. Peloquin, M. Brynda, M. Sugiura, S. Un, R. D. Britt and B. A. Diner, *J. Am. Chem. Soc.*, 2009, **131**, 4425–4433.
245 E. Schleicher, R. Bittl and S. Weber, *FEBS J*, 2009, **276**, 4290–4303.
246 C. W. M. Kay, H. El Mkami, G. Molla, L. Pollegioni and R. R. Ramsay, *J. Am. Chem. Soc.*, 2007, **129**, 16091–16097.
247 C. W. M. Kay, R. Feicht, K. Schulz, P. Sadewater, A. Sancar, A. Bacher, K. Möbius, G. Richter and S. Weber, *Biochemistry*, 1999, **38**, 16740–16748.

248 M. R. Fuchs, E. Schleicher, A. Schnegg, C. W. M. Kay, J. T. Toörring, R. Bittl, A. Bacher, G. Richter, K. Möbius and S. Weber, *J. Phys. Chem. B*, 2002, **106**, 8885–8890.
249 C. W. M. Kay, R. Bittl, A. Bacher, G. Richter and S. Weber, *J. Am. Chem. Soc*., 2005, **127**, 10780–10781.
250 A. Schnegg, C. W. M. Kay, E. Schleicher, K. Hitomi, T. Todo, K. Möbius and S. Weber, *Mol. Phys*., 2006, **104**, 1627–1633.
251 A. Schnegg, A. Okafuji, A. Bacher, R. Bittl, M. Fischer, M. R. Fuchs, P. Hegemann, M. Joshi, C. W. M. Kay, G. Richter, E. Schleicher and S. Weber, *Appl. Magn. Reson*., 2006, **30**, 345–358.
252 B. Barquera, L. Ramirez-Silva, J. E. Morgan and M. J. Nilges, *J. Biol. Chem*., 2006, **281**, 36482–36491.
253 O. Juaréz, M. J. Nilges, P. Gillespie, J. Cotton and B. Barquera, *J. Biol. Chem*., 2008, **283**, 33162–33167.
254 O. Juaréz, J. E. Morgan, M. J. Nilges and B. Barquera, *Proc. Natl. Acad. Sci. U.S.A*., 2010, **107**, 12505–12510.
255 A. Okafuji, A. Schnegg, E. Schleicher, K. Möbius and S. Weber, *J. Phys. Chem. B*., 2008, **112**, 3568–3574.
256 S. E. J. Rigby, R. M. G. Hynson, R. R. Ramsay, A. W. Munro and N. S. Scrutton, *J. Biol. Chem*., 2005, **280**, 4627–4631.
257 R. V. Dunn, A. W. Munro, N. J. Turner, S. E. J. Rigby and N. S. Scrutton, *ChemBioChem*, 2010, **11**, 1228–1231.
258 E. Schleicher, R. Wenzel, M. Ahmad, A. Batschauer, L.-O. Essen, K. Hitomi, E. D. Getzoff, R. Bittl, S. Weber and A. Okafuji, *Appl. Magn. Reson*., 2010, **37**, 339–352.
259 D. E. Edmondson, *Biochem. Soc. Trans*., 1985, **13**, 593–600.
260 K. T. Yue, A. K. Bhattacharyya, V. R. Zhelyaskov and D. E. Edmondson, *Arch. Biochem. Biophys*., 1993, **300**, 178–185.
261 C. W. M. Kay and S. Weber, in *Electron Paramagnetic Resonance*, eds. B. C. Gilbert, M. J. Davies and D. M. Murphy, Royal Society of Chemistry, Cambridge, edition, 2002, Vol. **18**, pp. 222–253.
262 R. Bittl and S. Weber, *Biochim. Biophys. Acta*, 2005, **1707**, 117–126.
263 T. Biskup, E. Schleicher, A. Okafuji, G. Link, K. Hitomi, E. D. Getzoff and S. Weber, *Angew. Chem. Int. Ed*., 2009, **48**, 404–407.
264 P. J. Bratt, O. G. Poluektov, M. C. Thurnauer, J. Krzystek, L.-C. Brunel, J. Schrier, Y.-W. Hsiao, M. Zerner and A. Angerhofer, *J. Phys. Chem. B*., 2000, **104**, 6973–6977.
265 O. Burghaus, M. Plato, D. Bumann, B. Neumann, W. Lubitz and K. Möbius, *Chem. Phys. Lett*., 1991, **185**, 381–386.
266 O. G. Poluektov, M. C. Thurnauer, L.-C. Brunel, S. A. Zvyagin, C. Boyce, L. Walker and A. Angerhofer, *The g-Factor Anisotropy of Bacteriochlorophyll* $a^{\bullet+}$, National High Magnetic Field Laboratory, 2000.
267 S. Sinnecker, W. Koch and W. Lubitz, *J. Phys. Chem. B*., 2002, **106**, 5281–5288.
268 F. MacMillan, M. Rohrer, J. Krzystek, L.-C. Brunel and A. W. Rutherford, *Photosynth.: Mech. Eff., Proc. Int. Congr. Photosynth., 11th*, 1998, **2**, 715–718.
269 P. Faller, A. W. Rutherford and S. Un, *J. Phys. Chem. B*, 2000, **104**, 10960–10963.
270 K. V. Lakshmi, O. G. Poluektov, M. J. Reifler, A. M. Wagner, M. C. Thurnauer and G. W. Brudvig, *J. Am. Chem. Soc*., 2003, **125**, 5005–5014.
271 C. R. D. Lancaster and H. Michel, in *Handbook of Metalloproteins*, eds. A. Messerschmidt, R. Huber, T. Poulos and K. Wiegard, John Wiley, Chichester, 2001, Vol. **1**, pp. 119–135.

272 C. N. Hunter, F. Daldal, M. C. Thurnauer and J. T. Beatty, eds., *The Purple Phototrophic Bacteria*, Springer, Dordrecht, 2008.
273 J. P. Allen and G. Feher, *Proc. Natl. Acad. Sci. U.S.A.*, 1984, **81**, 4795–4799.
274 W. Wang, R. L. Belford, R. B. Clarkson, P. H. Davis, J. Forrer, M. J. Nilges, M. D. Timken, T. Walczak, M. C. Thurnauer, J. R. Norris, A. L. Morris and Y. Zhang, *Appl. Magn. Reson.*, 1994, **6**, 195–215.
275 M. Huber, J. T. Törring, M. Plato, U. Finck, W. Lubitz, R. Feick, C. C. Schenck and K. Möbius, in *Sol. Energy Mater. Sol. Cells*, Editon edn., 1995, vol. 38, pp. 119–126
276 M. R. Fuchs, A. Schnegg, M. Plato, C. Schulz, F. Muh, W. Lubitz and K. Möbius, *Chem. Phys.*, 2003, **294**, 371–384.
277 A. Schnegg, A. A. Dubinskii, M. R. Fuchs, Y. A. Grishin, E. P. Kirilina, W. Lubitz, M. Plato, A. Savitsky and K. Möbius, *Appl. Magn. Reson.*, 2007, **31**, 59–98.
278 K. Möbius, A. Savitsky, A. Schnegg, M. Plato and M. Fuchs, *Phys. Chem. Chem. Phys.*, 2005, **7**, 19–42.
279 S. V. Paschenko, P. Gast and A. J. Hoff, *Appl. Magn. Reson.*, 2001, **21**, 325–334.
280 N. S. Ponomarenko, O. G. Poluektov, E. J. Bylina and J. R. Norris, *Biochim. Biophys. Acta*, 2010, **1797**, 1617–1626.
281 M. Di Valentin, D. Malorni, A. L. Maniero, G. Agostini, G. Giacometti, A. Vianelli, C. Vannini, A. G. Cattaneo, L.-C. Brunel and D. Carbonera, *Photosynth. Res.*, 2002, **71**, 33–44.
282 A. N. Webber and W. Lubitz, *Biochim. Biophys. Acta*, 2001, **1507**, 61–79.
283 C. Teutloff, W. Hofbauer, S. G. Zech, M. Stein, R. Bittl and W. Lubitz, *Appl. Magn. Reson.*, 2001, **21**, 363–379.
284 Y. J. Li, M. G. Lucas, T. Konovalova, B. Abbott, F. MacMillan, A. Petrenko, V. Sivakumar, R. L. Wang, G. Hastings, F. F. Gu, J. van Tol, L. C. Brunel, R. Timkovich, F. Rappaport and K. Redding, *Biochemistry*, 2004, **43**, 12634–12647.
285 A. Petrenko, K. Redding and L. D. Kispert, *Chem. Phys. Lett.*, 2005, **406**, 327–331.
286 P. Dorlet, L. Xiong, R. T. Sayre and S. Un, *J. Biol. Chem.*, 2001, **276**, 22313–22316.
287 S. Weber, in *Electron Paramagnetic Resonance, A Specialist Periodical Report*, eds. B. C. Gilbert, M. J. Davies and K. A. McLauchlan, The Royal Society of Chemistry, London, edn., 2000, Vol. **17**, pp. 43–77.
288 W. Lubitz, in *Electron Paramagnetic Resonance, A Specialist Periodical Report*, eds. B. C. Gilbert, M. J. Davies and D. M. Murphy, The Royal Society of Chemistry, London, edn., 2004, Vol. **19**, pp. 174–242.
289 O. Burghaus, M. Plato, M. Rohrer, K. Möbius, F. Macmillan and W. Lubitz, *J. Phys. Chem.*, 1993, **97**, 7639–7647.
290 M. K. Bowman, M. C. Thurnauer, J. R. Norris, S. A. Dikanov, V. I. Gulin, A. M. Tyryshkin, R. I. Samoilova and Y. D. Tsvetkov, *Appl. Magn. Reson.*, 1992, **3**, 353–368.
291 O. Nimz, F. Lendzian, C. Boullais and W. Lubitz, *Appl. Magn. Reson.*, 1998, **13**, 255–274.
292 C. Teutloff, R. Bittl and W. Lubitz, *Appl. Magn. Reson.*, 2004, **26**, 5–21.
293 M. Knüpling, J. T. Törring and S. Un, *Chem. Phys.*, 1997, **219**, 291–304.
294 M. Kaupp, C. Remenyi, J. Vaara, O. L. Malkina and V. G. Malkin, *J. Am. Chem. Soc.*, 2002, **124**, 2709–2722.
295 J. R. Asher, N. L. Doltsinis and M. Kaupp, *J. Am. Chem. Soc.*, 2004, **126**, 9854–9861.
296 S. Kacprzak and M. Kaupp, *J. Phys. Chem. B*, 2004, **108**, 2464–2469.

297 S. Sinnecker, M. Flores and W. Lubitz, *Phys. Chem. Chem. Phys.*, 2006, **8**, 5659–5670.
298 W. Lubitz and G. Feher, *Appl. Magn. Reson.*, 1999, **17**, 1–48.
299 R. A. Isaacson, E. C. Abresch, F. Lendzian, C. Boullais, M. L. Paddock, C. Mioskowski, W. Lubitz and F. G., in *The Reaction Center of Photosynthetic Bacteria*, ed. M. E. Beyerle, Springer, Berlin, edn., 1995, pp. 353–368.
300 U. Heinen, L. M. Utschig, O. G. Poluektov, G. Link, E. Ohmes and G. Kothe, *J. Am. Chem. Soc.*, 2007, **129**, 15935–15946.
301 R. Calvo, E. C. Abresch, R. Bittl, G. Feher, W. Hofbauer, R. A. Isaacson, W. Lubitz, M. Y. Okamura and M. L. Paddock, *J. Am. Chem. Soc.*, 2000, **122**, 7327–7341.
302 R. Calvo, R. A. Isaacson, M. L. Paddock, E. C. Abresch, M. Y. Okamura, A. L. Maniero, L.-C. Brunel and G. Feher, *J. Phys. Chem. B*, 2001, **105**, 4053–4057.
303 A. van der Est, I. Sieckmann, W. Lubitz and D. Stehlik, *Chem. Phys.*, 1995, **194**, 349–359.
304 F. MacMillan, J. Hanley, L. van der Weerd, M. Knüpling, S. Un and A. W. Rutherford, *Biochemistry*, 1997, **36**, 9297–9303.
305 J. Niklas, B. Epel, M. L. Antonkine, S. Sinnecker, M. E. Pandelia and W. Lubitz, *J. Phys. Chem. B*, 2009, **113**, 10367–10379.
306 J. Niklas, O. Gopta, B. Epel, W. Lubitz and M. L. Antonkine, *Appl. Magn. Reson.*, 2010, **38**, 187–203.
307 S. Santabarbara, M. Chen, A. W. D. Larkum and M. C. W. Evans, *FEBS Lett.*, 2007, **581**, 1567–1571.
308 F. MacMillan, F. Lendzian, G. Renger and W. Lubitz, *Biochemistry*, 1995, **34**, 8144–8156.
309 S. Grimaldi, P. Lanciano, P. Bertrand, F. Blasco and B. Guigliarelli, *Biochemistry*, 2005, **44**, 1300–1308.
310 R. Arias-Cartin, S. Lyubenova, P. Ceccaldi, T. Prisner, A. Magalon, B. Guigliarelli and S. Grimaldi, *J. Am. Chem. Soc.*, 2010, **132**, 5942–5943.
311 S. Grimaldi, R. Arias-Cartin, P. Lanciano, S. Lyubenova, B. Endeward, T. F. Prisner, A. Magalon and B. Guigliarelli, *J. Biol. Chem.*, 2010, **285**, 179–187.
312 S. M. Yi, K. V. Narasimhulu, R. I. Samoilova, R. B. Gennis and S. A. Dikanov, *J. Biol. Chem.*, 2010, **285**, 18241–18251.
313 S. Grimaldi, T. Ostermann, N. Weiden, T. Mogi, H. Miyoshi, B. Ludwig, H. Michel, T. F. Prisner and F. Macmillan, *Biochemistry*, 2003, **42**, 5632–5639.
314 T. M. Lin, R. I. Samoilova, R. B. Gennis and S. A. Dikanov, *J. Am. Chem. Soc.*, 2008, **130**, 15768–15769.
315 F. MacMillan, C. Lange, M. Bawn and C. Hunte, *Appl. Magn. Reson.*, 2010, **37**, 305–316.
316 S. A. Dikanov, J. T. Holland, B. Endeward, D. R. J. Kolling, R. I. Samoilova, T. F. Prisner and A. R. Crofts, *J. Biol. Chem.*, 2007, **282**, 25831–25841.
317 C. W. M. Kay, B. Mennenga, H. Görisch and R. Bittl, *Proc. Natl. Acad. Sci. U.S.A.*, 2006, **103**, 5267–5272.
318 B. Mennenga, C. W. M. Kay and H. Görisch, *Arch. Microbiol.*, 2009, **191**, 361–367.
319 C. W. M. Kay, B. Mennenga, H. Görisch and R. Bittl, *FEBS Lett.*, 2004, **564**, 69–72.
320 C. W. M. Kay, B. Mennenga, H. Görisch and R. Bittl, *J. Am. Chem. Soc.*, 2005, **127**, 7974–7975.
321 C. W. M. Kay, B. Mennenga, H. Görisch and R. Bittl, *J. Biol. Chem.*, 2006, **281**, 1470–1476.
322 S. Weber and R. Bittl, *Bull. Chem. Soc. Jpn.*, 2007, **80**, 2270–2284.

323 R. de Beer, D. van Ormondt, M. A. van Ast, R. Banen, J. A. Duine and J. Frank, *J. Chem. Phys*., 1979, **70**, 4491–4495.
324 A. Sato, K. Takagi, K. Kano, N. Kato, J. A. Duine and T. Ikeda, *Biochem. J*, 2001, **357**, 893–898.
325 S. Gómez-Manzo, A. Solano-Peralta, J. P. Saucedo-Vázquez, J. E. Escamilla-Marván, P. M. H. Kroneck and M. E. Sosa-Torres, *Biochemistry*, 2010, **49**, 2409–2415.
326 K. Kobayashi, G. Mustafa, S. Tagawa and M. Yamada, *Biochemistry*, 2005, **44**, 13567–13572.
327 C. Anthony, *Arch. Biochem. Biophys*., 2004, **428**, 2–9.
328 J. Hanley, Y. Deligiannakis, A. Pascal, P. Faller and A. W. Rutherford, *Biochemistry*, 1999, **38**, 8189–8195.
329 Y. Gao, K. E. Shinopoulos, C. A. Tracewell, A. L. Focsan, G. W. Brudvig and L. D. Kispert, *J. Phys. Chem. B*, 2009, **113**, 9901–9908.
330 A. R. Hurshman, C. Krebs, D. E. Edmondson, B. H. Huynh and M. A. Marletta, *Biochemistry*, 1999, **38**, 15689–15696.
331 P. P. Schmidt, R. Lange, A. C. F. Gorren, E. R. Werner, B. Mayer and K. K. Andersson, *J. Biol. Inorg. Chem*., 2001, **6**, 151–158.
332 S. Stoll, Y. NejatyJahromy, J. J. Woodward, A. Ozarowski, M. A. Marletta and R. D. Britt, *J. Am. Chem. Soc*., 2010, **132**, 11812–11823.
333 C.-C. Wei, Z.-Q. Wang, J. Tejero, Y.-P. Yang, C. Hemann, R. Hille and D. J. Stuehr, *J. Biol. Chem*., 2008, **283**, 11734–11742.
334 P. A. Frey, A. D. Hegeman and F. J. Ruzicka, *Crit. Rev. Biochem. Molec. Biol*., 2008, **43**, 63–88.
335 O. T. Magnusson, G. H. Reed and P. A. Frey, *Biochemistry*, 2001, **40**, 7773–7782.
336 A. P. Bussandri, C. W. Kiarie and H. van Willigen, *Res. Chem. Intermed*., 2002, **28**, 697–710.
337 V. F. Bouchev, C. M. Furdui, S. Menon, R. B. Muthukumaran, S. W. Ragsdale and J. McCracken, *J. Am. Chem. Soc*., 1999, **121**, 3724–3729.
338 E. Chabriere, C. Vernede, B. Guigliarelli, M. H. Charon, E. C. Hatchikian and J. C. Fontecilla-Camps, *Science*, 2001, **294**, 2559–2563.
339 G. M. Sandala, D. M. Smith, M. L. Coote, B. T. Golding and L. Radom, *J. Am. Chem. Soc*., 2006, **128**, 3433–3444.
340 G. J. S. Lohman, G. J. Gerfen and J. Stubbe, *Biochemistry*, 2010, **49**, 1396–1403.
341 X. Li, J. Telser, R. C. Kunz, B. M. Hoffman, G. J. Gerfen and S. W. Ragsdale, *Biochemistry*, 2010, **49**, 6866–6876.
342 D. I. Kern, M. Goenrich, B. Jaun, R. K. Thauer, J. Harmer and D. Hinderberger, *J. Biol. Inorg. Chem*., 2007, **12**, 1097–1105.
343 S. Ebner, B. Jaun, M. Goenrich, R. K. Thauer and J. Harmer, *J. Am. Chem. Soc*., 2010, **132**, 567–575.
344 Y. Zhang, X. Zhu, A. T. Torelli, M. Lee, B. Dzikovski, R. M. Koralewski, E. Wang, J. Freed, C. Krebs, S. E. Ealick and H. Lin, *Nature*, 2010, **465**, 891–896.
345 R. M. Cicchillo, H. Zhang, J. A. V. Blodgett, J. T. Whitteck, G. Li, S. K. Nair, W. A. van der Donk and W. W. Metcalf, *Nature*, 2009, **459**, 871–874.
346 B. Brogioni, D. Biglino, A. Sinicropi, E. J. Reijerse, P. Giardina, G. Sannia, W. Lubitz, R. Basosi and R. Pogni, *Phys. Chem. Chem. Phys*., 2008, **10**, 7284–7292.
347 N. S. Lees, D. Chen, C. J. Walsby, E. Behshad, P. A. Frey and B. M. Hoffman, *J. Am. Chem. Soc*., 2006, **128**, 10145–10154.
348 S. K. Jackson, J. T. Hancock and P. E. James, in *Electron Paramagnetic Resonance, A Specialist Periodical Report*, eds. B. C. Gilbert, M. J. Davies and

D. M. Murphy, The Royal Society of Chemistry, London, edn. , 2007, Vol. **20**, pp. 192–244.
349 M. A. Yu, T. Egawa, S.-R. Yeh, D. L. Rousseau and G. J. Gerfen, *J. Magn. Reson.*, 2010, **203**, 213–219.
350 M. Witwicki, M. Jerzykiewicz, A. R. Jaszewski, J. Jezierska and A. Ozarowski, *J. Phys. Chem. A*, 2009, **113**, 14115–14122.
351 M. Witwicki, J. Jezierska and A. Ozarowski, *Chem. Phys. Lett.*, 2009, **473**, 160–166.
352 S. Panagiota, M. Louloudi and Y. Deligiannakis, *Chem. Phys. Lett.*, 2009, **472**, 85–89.
353 M. D. Sevilla and D. Becker, in *Electron Paramagnetic Resonance, A Specialist Periodical Report*, eds. B. C. Gilbert, M. J. Davies and D. M. Murphy, The Royal Society of Chemistry, London, edn., 2004, Vol. **21**, pp. 243–278.
354 D. Becker and M. D. Sevilla, in *Electron Paramagnetic Resonance, A Specialist Periodical Report*, eds. B. C. Gilbert, M. J. Davies and D. M. Murphy, The Royal Society of Chemistry, London, edn., 2008, Vol. **21**, pp. 33–58.
355 A. Adhikary, A. Kumar, D. Becker and M. D. Sevilla, *J. Phys. Chem. B*, 2006, **110**, 24171–24180.
356 A. Adhikary, D. Khanduri and M. D. Sevilla, *J. Am. Chem. Soc.*, 2009, **131**, 8614–8619.
357 M. A. Tarpan, H. Vrielinck, H. De Cooman and F. Callens, *J. Phys. Chem. A*, 2009, **113**, 7994–8000.
358 H. De Cooman, E. Pauwels, H. Vrielinck, E. Sagstuen, M. Waroquier and F. Callens, *J. Phys. Chem. B*, 2010, **114**, 666–674.
359 E. R. Georgieva, L. Pardi, G. Jeschke, D. Gatteschi, L. Sorace and N. D. Yordanov, *Free Radical Res.*, 2006, **40**, 553–563.
360 M. Wencka, K. Wichlacz, H. Kasprzyk, S. Lijewski and S. K. Hoffmann, *Cellulose*, 2007, **14**, 183–194.
361 A. Engalytcheff, M. Kolberg, A.-L. Barra, K. K. Andersson and B. Tilquin, *Free Radical Res.*, 2004, **38**, 59–66.